

AD-774 395

DIFFERENTIAL GAME BARRIERS FOR TWO
SPACECRAFT ENGAGED IN A PURSUIT -
EVASION GAME IN ORBIT

Victor W. Grazier

Air Force Institute of Technology

Prepared for:

Air Force Flight Dynamics Laboratory

December 1973

DISTRIBUTED BY:

NTIS

National Technical Information Service
U. S. DEPARTMENT OF COMMERCE
5285 Port Royal Road, Springfield Va. 22151

Unclassified

Security Classification

AD 774395

DOCUMENT CONTROL DATA - R & D

(Security classification of title, body of abstract and indexing notation must be entered when the overall report is classified)

ORIGINATING ACTIVITY (Corporate author)

Air Force Institute of Technology
Wright-Patterson AFB, Ohio 45433

2a. REPORT SECURITY CLASSIFICATION

Unclassified

2b. GROUP

3. REPORT TITLE

Differential Game Barriers for Two Spacecraft Engaged in a Pursuit-Evasion Game in Orbit

4. DESCRIPTIVE NOTES (Type of report and inclusive dates)

AFIT Thesis

5. AUTHOR(S) (First name, middle initial, last name)

Victor W. Grazier, Captain, USAF

6. REPORT DATE

December 1973

7a. TOTAL NO. OF PAGES

81

7b. NO. OF REFS

6

8a. CONTRACT OR GRANT NO.

N/A

9a. ORIGINATOR'S REPORT NUMBER(S)

GA/NC/73A-3

9b. PROJECT NO.

c.

9c. OTHER REPORT NO(S) (Any other numbers that may be assigned this report)

d.

10. DISTRIBUTION STATEMENT

Approved for public release; distribution unlimited.

Approved for public release; IAW AFR 190-17 ¹² SPONSORING MILITARY ACTIVITY
Approved for public release; IAW AFR 190-17 Air Force Flight Dynamics Laboratory
JERRY C. AIX, Captain, USAF Wright-Patterson AFB, Ohio
Director of Information

11. ABSTRACT This study, searches for the differential game barrier for two spacecraft engaged in a pursuit-evasion game in orbit. By linearizing the equations of motion, a set of linear state equations is developed which, along with the non-linear state equations, is used to generate trajectories backward from the terminal surface. These trajectories for the linear and non-linear equations are then compared for equivalence and also used to provide necessary information on the barrier itself. Once the barrier has been determined, a method is developed theoretically to evaluate the location of a given starting point as to whether it lies in the escape zone or in the capture zone. The computer programs used in this study are included in the appendix for future research in this area.

Reproduced by
NATIONAL TECHNICAL
INFORMATION SERVICE
U.S. Department of Commerce
Springfield, VA 22151

DD FORM 1 NOV 63 1473

Unclassified

Security Classification

DIFFERENTIAL GAME BARRIERS FOR
TWO SPACECRAFT ENGAGED IN A
PURSUIT-EVASION GAME
IN ORBIT

THESIS

GA/MC/73A-3

Victor W. Grazier
Captain USAF

DDC
FEB 22 1974
REF ID: A6521
B

Approved for public release;
distribution unlimited.

16

Unclassified

Security Classification

AD774395

14	KEY WORDS	LINK A		LINK B		LINK C	
		ROLE	WT	ROLE	WT	ROLE	WT
	Differential Games						
	Barriers						
	Pursuit-Evasion						
	Trajectory Optimization						
	Near-Earth Orbit						

ia

Unclassified

Security Classification

DIFFERENTIAL GAME BARRIERS FOR TWO SPACECRAFT
ENGAGED IN A PURSUIT-EVASION GAME
IN ORBIT

THESIS

Presented to the Faculty of the School of Engineering
of the Air Force Institute of Technology
Air University
in Partial Fulfillment of the
Requirements for the Degree of
Master of Science
by

Victor W. Grazier, B.S.E.S.
Captain USAF

Graduate Astronautics

December 1973

Approved for public release; distribution unlimited.

Preface

This thesis represents my attempts to determine the differential game barrier for two spacecraft in near-earth orbit. The vehicle parameters are in general viewed in two dimensions while the barrier, due to the dimensionality of the linear state equations, is constructed in four dimensions. Once determined, the barrier is analyzed to determine whether it divides the playing space into two separate zones: an escape zone and a capture zone.

I would like to express my sincere appreciation to the faculty of the Air Force Institute of Technology for their assistance in the research and preparation of this thesis. I would especially like to thank my advisor, Major Gerald M. Anderson, for his guidance and suggestions toward the completion of this study and also Professor Edstrom of the Mathematics Department for devoting his time to helping solve many differential equation problems. I also want to express my heartfelt gratitude to my wife, Marsha, for her undying devotion, unfailing enthusiasm, and unceasing encouragement. Also, I want to thank the Lord for this opportunity He has provided and for His invaluable guidance, insight, and motivation without which this study would not have been completed.

Victor W. Grazier

Contents

	Page
Preface	ii
List of Figures and Tables	v
List of Symbols	vi
Abstract	viii
I. Introduction	1
Background	1
Problem	1
Current Knowledge	2
Scope	3
Assumptions	3
Approach	4
II. General Equation Development	5
Nonlinear Equations of Motion	5
Linearized Equations of Motion	6
Normalizing the Variables	8
Non-linear Normalization	8
III. Differential Game Barrier Formulation	11
Theory	11
Games of Kind	13
The Barrier Development	14
Non-linear Equation Development	15
Linear Equation Development	18
Terminal Conditions	24
Non-linear Development	24
Linear Development	28
IV. Methods of Solving the Linear Equations	31
The Costate Equations	31
The State Equations	32

Contents (Continued)

	Page
V. Analysis of the Barrier	36
The Linear Program	37
The Non-linear Program	38
Equivalence	40
Starting Point Locations	41
VI. Conclusions and Recommendations	45
Conclusions	45
Recommendations	50
Bibliography	54
Appendix A: Sine and Cosine Approximations	55
Appendix B: Non-linear Integration Program	66
Vita	73

List of Figures

Figure	Page
1 Orbital Geometry	6
2 Linearized Geometry	20
3 Terminal Surface Parameters	25
4 Boundary of the Usable Part and Barrier Portion, 0 to 90 Degrees	46
5 Boundary of the Usable Part, 90 to 180 Degrees.	47
6 Boundary of the Usable Part, 180 to 270 Degrees	48
7 Boundary of the Usable Part, 270 to 360 Degrees	49
8 Barrier Cut at $Y_2/Y_3 = -1.00$	51
9 Barrier Cut at $Y_2/Y_3 = +1.00$	52

List of Tables

Table

1 Equivalence Values, $\phi = 355$ Degrees	42
--	----

List of Symbols

<u>Symbols</u>	<u>Definition</u>
r	radius from the earth's center
r_0	radius of circular reference orbit
v_θ	tangential velocity
v_r	radial velocity
v_0	velocity of circular reference orbit
θ	angular position of spacecraft measured from some arbitrary reference in the orbital plane
T	thrust
m	mass
X	state variable
Y	relative difference state variable
μ	earth's gravitational constant
t	time
τ	non-dimensional time, $\tau = \frac{v_0 t}{r_0}$
τ_1	non-dimensional time for backward integration
R	radius of the terminal surface
U	normalized thrust, $U = \frac{r_0 T}{m v_0^2}$
λ	costate variable
H	Hamiltonian function
H_B	barrier Hamiltonian

List of Symbols (Continued)

<u>Symbols</u>	<u>Definition</u>
α	thrust (control) angle measured counterclockwise from the player's local horizontal
ϕ	angle around the terminal surface measured counterclockwise from the pursuer's local horizontal
ν	vector normal to the terminal surface
J	payoff function
g	acceleration due to gravity, taken as 32.2 ft/sec
TPBVP	two point boundary value problem

Subscripts

E	denotes the evader
P	denotes the pursuer
f	denotes the final condition

Superscripts

\cdot	denotes derivative with respect to time
\cdot	denotes derivative with respect to τ , the non-dimensional time

I. Introduction

Background

The advent of the space age has thrust man into orbital space-craft and outward to the moon. This intense activity in space has made it seem inevitable that man would arm his space vehicles in an effort to gain power or influence on earth. In an effort to preclude such actions, many nations joined together in signing the Treaty of 1967, an agreement to keep space neutral. Although man's intentions were commendable, the past has shown dramatically that dreams of power can overcome any barriers, and unfortunately, the barrier to arms in space must be viewed in this light. While vigorously supporting the efforts to keep space neutral, the United States must continue its research in the area of orbital defenses in the eventuality that some aggressive government attempts to gain control of the space around the earth.

Problem

This study investigates the region surrounding two orbital spacecraft engaged in a pursuit-evasion game. In this game, the pursuer desires capture while the evader desires to escape. Termination, then, if it is possible, results when the pursuer forces the evader to come within a specified distance of him. This distance is the radius of the terminal surface which is centered on the pursuer. From this surface, trajectories are generated backward in time in

order to provide information concerning another surface known as the "barrier."

The barrier is a surface which results from the application of differential game theory. This surface generally divides the playing space of interest into two zones: a capture zone and an escape zone. Starting points from which capture can not occur lie in the escape zone. Those from which escape is not possible lie in the capture zone. Starting points on the barrier itself will remain on the barrier for a neutral outcome as long as both players use their optimal strategies.

Current Knowledge

The use of differential game theory in numerous fields of endeavor began in earnest in the late 1950's. A major contributor to this theory was Rufus Isaacs (Ref 1). Although differential game theory has been investigated extensively over the past decade for applications to air-to-air engagements, relatively little work has been done on the use of this theory for orbiting spacecraft. R. E. Wong (Ref 2) used differential game techniques to investigate fixed time, minimum final separation, assuming that the encounter took place in a constant gravity field. In his master's thesis, R. H. Woodward (Ref 3) investigated the free time, minimum final distance problem in an inverse square gravity field. To date, no one has investigated differential game barriers for two spacecraft in orbit.

Scope

The construction of the barrier requires numerous assumptions (some of which are listed in the next section) along with many approximations. These are necessary to reduce the dimensionality of the problem to something that can be handled, while also removing complexities that do not greatly affect the outcome of the problem. In this manner, the closed-form solutions may be found which ultimately will allow analysis of the barrier itself. Once the barrier has been constructed, the objective is to analyze this barrier to define the conditions necessary for establishing where each starting point is located. In other words, by applying these conditions, it should be possible to determine whether given starting points are in the escape or the capture zone. Surely other objectives could be sought; however, due to time limitations, this study will concentrate only on the above search.

Assumptions

1. Both vehicles thrust continuously. If the evader stopped thrusting, capture could readily occur. If the pursuer quit thrusting, the evader could rapidly escape.
2. This pursuit-evasion game takes place in an inverse-square gravity field.
3. Both vehicles have constant mass. This entails the further assumptions that the time period for the pursuit-evasion game is

sufficiently short and that the thrust is very low. Variable mass, however, would be an area for further investigation in future studies.

4. Control is provided by varying the thrust vector direction. The control angle itself is measured from each vehicle's local horizontal.

5. Each player has perfect knowledge of the position and capabilities of his opponent. Otherwise, the game would degenerate with one player holding an obvious advantage.

Approach

1. Linearize the equations of motion about a circular reference orbit.

2. Normalize both the linear and non-linear equations of motion about the same circular reference orbit. Use normalized time to develop the linear and non-linear state equations.

3. Apply necessary conditions to establish boundary conditions for both the linear and non-linear equations.

4. Compare linear trajectories with corresponding non-linear trajectories in order to determine the validity of the linear approximation.

5. Vary parameters around the terminal surface and out the trajectories in order to gain information on the barrier.

6. Develop a method to determine whether each given starting point lies in the escape zone, in the capture zone, or on the barrier itself.

II. General Equation Development

The objectives of this chapter are first to develop the general equations of motion for a spacecraft in orbit, then to linearize these equations about a circular reference orbit, and finally to normalize them about this same reference orbit.

Nonlinear Equations of Motion

Assuming that the earth is spherical and then using a polar coordinate system, the equations of motion for a spacecraft in orbit, as found in any basic dynamics textbook, are as follows:

$$\ddot{r} - r\dot{\theta}^2 = -\frac{\mu}{r^2} + \frac{T \sin \alpha}{m} \quad (1)$$

$$r\ddot{\theta} + 2\dot{r}\dot{\theta} = \frac{T \cos \alpha}{m} \quad (2)$$

where α is the angle between the thrust vector and the local horizontal as in Fig. 1.

In order to work with these equations, it is desirable to transform them into expressions concerning the tangential and radial velocities, v_θ and v_r respectively. This can be accomplished by using the following relationships.

$$v_\theta = r\dot{\theta} \quad (3a)$$

$$v_r = \dot{r} \quad (3b)$$

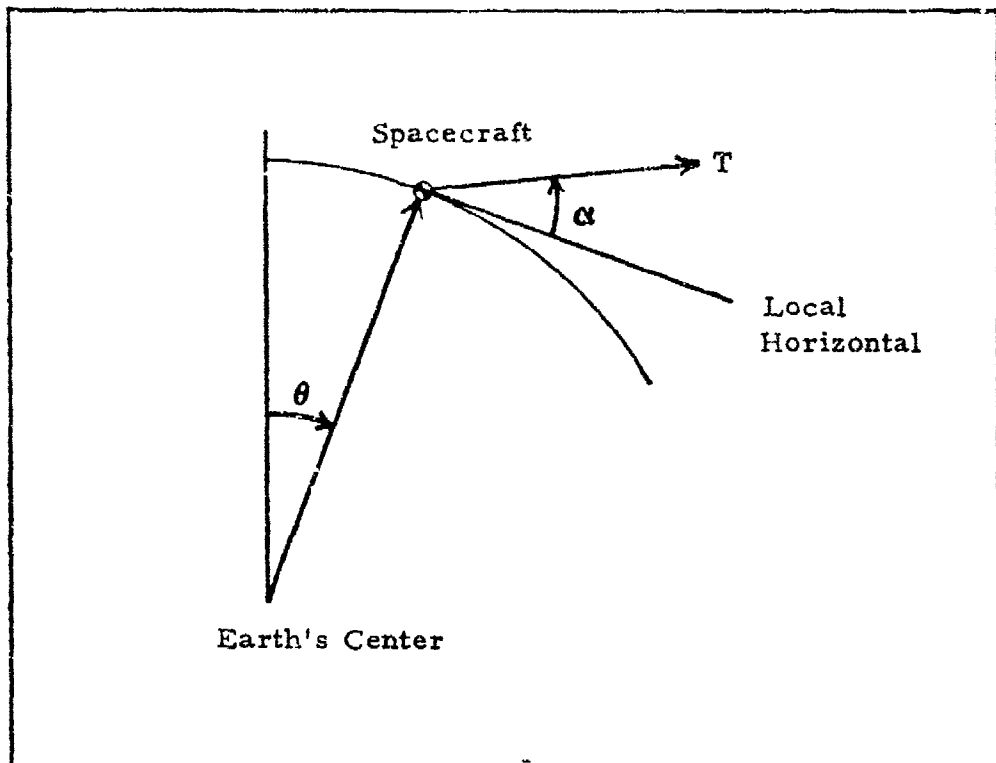


Fig. 1. Orbital Geometry

Through differentiation, expressions for \dot{r} , $\dot{\theta}$, \dot{v}_r and \dot{v}_θ may be obtained which, when substituted into Eqs. (1) and (2), yield these equations of motion.

$$\dot{v}_r - \frac{v_\theta^2}{r} = -\frac{\mu}{r^2} + \frac{T \sin \alpha}{m} \quad (4a)$$

$$\dot{v}_\theta + \frac{v_r v_\theta}{r} = \frac{T \cos \alpha}{m} \quad (4b)$$

Linearized Equations of Motion

Linearizing Eqs. (3) and (4) about a circular reference orbit yields

$$\Delta \dot{r} = \Delta v_r \quad (5a)$$

$$\Delta \dot{\theta} = \frac{\Delta v_\theta}{r} - \frac{v_\theta \Delta r}{r^2} \quad (5b)$$

as well as

$$\Delta \dot{v}_r - \frac{2v_\theta \Delta v_\theta}{r} + \frac{v_\theta^2 \Delta r}{r^2} - \frac{2\mu \Delta r}{r^3} = \frac{T \sin \alpha}{m} \quad (6)$$

$$\Delta \dot{v}_\theta + \frac{\Delta v_r v_\theta}{r} + \frac{v_r \Delta v_\theta}{r} - \frac{v_r v_\theta \Delta r}{r^2} = \frac{T \cos \alpha}{m} \quad (7)$$

In these equations the terms v_r , v_θ , and r now refer to the reference orbit. The delta terms refer to deviations from the reference orbit for these given parameters.

Assuming that the reference orbit for linearization is circular,

$$v_r = 0 \quad \text{and} \quad r \dot{\theta}^2 = \frac{\mu}{r^2} \quad (8a)$$

or

$$v_\theta^2 = \frac{\mu}{r} \quad (8b)$$

Substituting these expressions into Eqs. (6) and (7) gives the following linearized equations of motion.

$$\Delta \dot{v}_r = \frac{2v_\theta \Delta v_\theta}{r} + \frac{v_\theta^2 \Delta r}{r^2} + \frac{T \sin \alpha}{m} \quad (9)$$

$$\Delta \dot{v}_\theta = - \frac{\Delta v_r v_\theta}{r} + \frac{T \cos \alpha}{m} \quad (10)$$

Normalizing the Variables

At this point it is desirable to normalize the parameters about a circular orbit, with radius r_0 and velocity V_0 , so that significant figures are not lost due to large differences in magnitude between these parameters. The velocity magnitude may be several miles per second while the radii may be thousands of miles.

In order to work with the non-dimensional parameters, especially regarding the state equation development, it is necessary to introduce a non-dimensional time parameter τ defined by

$$\tau = \frac{V_0}{r_0} t \quad . \quad (11)$$

By means of the chain rule for differentiation,

$$\frac{d(\)}{d\tau} = \frac{d(\)}{dt} \frac{dt}{d\tau} = \frac{r_0}{V_0} \frac{d(\)}{dt} \quad (12)$$

In this manner, $\frac{dV_r}{d\tau} = V_r'$, where the prime represents differentiation with respect to τ .

Non-linear Normalization

Define the following normalized state variables.

$$x_1 = \frac{r}{r_0} \quad (13a)$$

$$x_2 = \frac{V_r}{V_0} \quad (13b)$$

$$x_3 = \frac{V_\theta}{V_0} \quad (13c)$$

$$X_4 = \theta \quad (13d)$$

By use of Eq. (12), the following normalized, non-linear equations of motion are determined.

$$X'_1 = X_2 \quad (14a)$$

$$\frac{d(X_2)}{d\tau} = \frac{r_0}{v_0} \left[\frac{\dot{v}_r}{v_0} \right] = \frac{r_0}{v_0^2} \left[\frac{v_\theta^2}{r} - \frac{\mu}{r^2} + \frac{T \sin \alpha}{m} \right]$$

For the normalizing orbit, $\mu = v_0^2 r_0$, so that

$$X'_2 = \frac{X_3^2}{X_1} - \frac{1}{X_1^2} + U \sin \alpha \quad (14b)$$

where $U = \frac{r_0 T}{v_0^2 m}$, a constant with thrust T and mass m . Differentiation of Eqs. (13c) and (13d) with respect to τ yield the remaining

non-linear state equations.

$$X'_3 = - \frac{X_2 X_3}{X_1} + U \cos \alpha \quad (14c)$$

$$X'_4 = \frac{X_3}{X_1} \quad (14d)$$

To this point the general equation development has followed closely the work of R. H. Woodward (Ref 3). In order to avoid

repetition and since the normalized, linear equations involve terms for both the pursuer and the evader, this development will be included in the next chapter along with the differential game barrier theory.

III. Differential Game Barrier Formulation

This chapter presents the theory and equations of the differential game barrier formulation for a pursuer and evader engaged in a pursuit-evasion game in orbit.

Theory

This section must, of necessity, follow closely the work of others. The nomenclature and theory of both Isaacs (Ref 1) and Bryson and Ho (Ref 4) are combined, with the resulting development being very similar to that used by P. H. Cawdery (Ref 5).

The objective of this development is to find the minimax solution, if one exists, to the expression

$$J = \phi[\underline{X}(t_f)] \quad (15)$$

with n-dimensional state vector of the type

$$\dot{\underline{X}} = f[\underline{X}, u, v, t]; \underline{X}(t_0) = \underline{X}_0 \quad (16)$$

and terminal constraints

$$\psi[\underline{X}(t_f)] = 0 \quad (17)$$

In Eq. (16) u and v represent the controls associated with the pursuer, P , and the evader, E , respectively. The aim is to determine the pair, u^* and v^* , such that

$$J(u^*, v) \leq J(u^*, v^*) \leq J(u, v^*) \quad (18)$$

According to Isaacs, the saddle point solution, $J(u^*, v^*)$, is the value of the game. The necessary conditions for this solution, called the solution in the small, are

$$H(\underline{X}, \underline{\lambda}, u, v, t) = \underline{\lambda}^T \underline{f} \quad (19)$$

$$\underline{\lambda}^T = - H_{\underline{X}}(\underline{X}, \underline{\lambda}, u, v, t) \quad (20)$$

where H is defined as the Hamiltonian and $\underline{\lambda}$ is the costate vector.

The n -dimensional costate vector $\underline{\lambda}$ is subject to the following transversality conditions.

$$\underline{\lambda}(t_f) = \phi_{\underline{X}}(t_f) + \nu \psi_{\underline{X}}(t_f) \quad (21)$$

$$H(t_f) = \phi_t(t_f) + \nu \psi_t(t_f) \quad (22)$$

where ν is a Lagrange multiplier.

In order to determine the optimal controls, H , of Eq. (20), must be minimized with respect to control u and maximized with respect to v so that

$$H^* = \max_v \min_u H(\underline{X}, \underline{\lambda}, u, v, t) \quad (23)$$

In order for the solution to exist, H must be assumed to be separable. In this case

$$\max_v \min_u H = \min_u \max_v H \quad (24)$$

For this problem H is assumed to be separable. This means that H does not have terms containing both u and v together. This insures a saddle point solution as stated in Eq. (18) with u^* minimizing and v^* maximizing. In addition, if t does not explicitly appear in Eq. (19), then H , ϕ , and ψ are not dependent on time thereby yielding the following important result from Eq. (22).

$$H(t) = H(t_f) = 0 \quad (25)$$

Games of Kind

Isaacs (Ref 1) introduces two types of differential games: games of degree and games of kind. In the former, which may be contained within a game of kind, the players attempt to maximize or minimize the final payoff as a function of the variables of the game. In this type of game the payoff is not determined until termination, thus presuming that the game does actually end. In games of kind the essential problem is the achievement of termination itself where one player desires termination while the other does not.

Termination in Isaacs' game of kind is taken to mean either that the evader is forced to come within a certain proximity of the pursuer or a long time period elapses without capture occurring. The proximity has been formalized in the playing space into a surface C which is defined as the terminal surface. For capture to occur, then,

the evader must be forced not only to this surface but also to penetrate it. Capture, escape, and a third result, that of a neutral outcome, are explained more fully below.

In this thesis the pursuer P desires termination or capture whereas the evader E desires to avoid termination, thus to escape, or at least to delay capture as long as possible. The outcomes of the game of kind then fall into three general categories:

- a. P can capture for all starting positions in the playing space.
- b. E can escape for all starting positions.
- c. Neither P can capture nor E can escape for all starting positions: a neutral outcome.

Category c is the one of interest in this thesis since the result demands that both P and E play optimally. If P were to momentarily play nonoptimally, E could force P out of a neutral outcome and escape. Likewise, if E were to play nonoptimally, capture would result. Therefore, the playing space is divided into two zones, capture and escape, by a surface which contains all starting points for which the outcome is neutral. This surface, then, is defined as the barrier.

The Barrier Development

The condition that must be met for a barrier to exist is as follows:

$$\min_u \max_v \sum_{i=1}^n v_i f_i(X, u, v) = 0 \quad (26)$$

where ν represents a vector normal to the terminal surface. This relationship will be called the Barrier Hamiltonian, a term borrowed from P. H. Cawdery (Ref 5), and is represented by H_B . Since the ν vector dotted into f equals zero, where f equals the velocity \dot{X} , the two vectors must be orthogonal. Therefore, at that point on the terminal surface, the component of the velocity in the direction of ν is zero, thus penetration can not occur. Points which meet this criteria have been classified by Isaacs as the boundary of the usable part (BUP). The usable part, where Eq. (26) is less than zero, defines the portion of the terminal surface where the pursuer P can force termination. Obviously, then, the nonusable part is that portion of the terminal surface where Eq. (26) is greater than zero. At these points, the evader E can frustrate termination and thus escape; therefore, this portion is nonusable.

The construction of the barrier involves starting with the initial conditions at the terminal surface and integrating the state and costate equations backwards in time. The resulting trajectories provide points required for constructing the barrier.

Non-linear Equation Development

The non-linear equations, presented earlier as Eqs. (14), are repeated below in the differential game format for the evader. The equations are identical for both players with only the (E) or (P) subscripts to differentiate between the two.

$$x'_{1E} = x_{2E} \quad (27a)$$

$$x'_{2E} = \frac{x_{3E}^2}{x_{1E}} - \frac{1}{x_{1E}^2} + U_E \sin \alpha_E \quad (27b)$$

$$x'_{3E} = -\frac{x_{2E}x_{3E}}{x_{1E}} + U_E \cos \alpha_E \quad (27c)$$

$$x'_{4E} = \frac{x_{3E}}{x_{1E}} \quad (27d)$$

A like set of equations exists for the pursuer with the subscript (E) replaced by (P).

The Hamiltonian, then, is formed by adjoining the costates to the state equations.

$$\begin{aligned}
 H = & \lambda_{1E} x_{2E} + \lambda_{2E} \left[\frac{x_{3E}^2}{x_{1E}} - \frac{1}{x_{1E}^2} + U_E \sin \alpha_E \right] \\
 & + \lambda_{3E} \left[-\frac{x_{2E}x_{3E}}{x_{1E}} + U_E \cos \alpha_E \right] + \lambda_{4E} \frac{x_{3E}}{x_{1E}} \\
 & + \lambda_{1P} x_{2P} + \lambda_{2P} \left[\frac{x_{3P}^2}{x_{1P}} - \frac{1}{x_{1P}^2} + U_P \sin \alpha_P \right] \\
 & + \lambda_{3P} \left[-\frac{x_{2P}x_{3P}}{x_{1P}} + U_P \cos \alpha_P \right] + \lambda_{4P} \frac{x_{3P}}{x_{1P}} \quad (28)
 \end{aligned}$$

From this equation the barrier costate equations may be determined by applying the necessary conditions from Eqs. (20).

$$\lambda'_{1E} = - \frac{dH}{dx_{1E}} = \frac{\lambda_{2E}x_{3E}^2}{x_{1E}^2} - \frac{2\lambda_{2E}}{x_{1E}^2} - \frac{\lambda_{3E}x_{2E}x_{3E}}{x_{1E}^2} + \frac{\lambda_{4E}x_{3E}}{x_{1E}^2} \quad (29a)$$

$$\lambda'_{2E} = -\lambda_{1E} + \frac{\lambda_{3E}x_{3E}}{x_{1E}} \quad (29b)$$

$$\lambda'_{3E} = - \frac{2\lambda_{2E}x_{3E}}{x_{1E}} + \frac{\lambda_{3E}x_{2E}}{x_{1E}} - \frac{\lambda_{4E}}{x_{1E}} \quad (29c)$$

$$\lambda'_{4E} = 0 \quad \text{yielding } \lambda_{4E} = \text{a constant} \quad (29d)$$

Again, a like set of equations exists for the pursuer with the subscript (E) replaced by (P).

The optimum barrier control angles for the pursuer's and the evader's thrust can be determined, as mentioned previously, by minimizing H with respect to u and maximizing it with respect to v, where α_P represents u and α_E represents v. After minimaxing H, the proper signs are determined by applying the following second partial derivative necessary conditions.

$$\frac{d^2H}{du^2} > 0 \quad \frac{d^2H}{dv^2} < 0 \quad (30)$$

The maximizing and minimizing of H, then, results in the following relationships.

$$\tan \alpha_E = \frac{\lambda_{2E}}{\lambda_{3E}} \quad (31)$$

and

$$\tan \alpha_P = \frac{\lambda_{2P}}{\lambda_{3P}} \quad (32)$$

By applying the conditions in Eqs. (30), the optimum barrier control angles are determined to be

$$\sin \alpha_E = \frac{+ \lambda_{2E}}{\sqrt{\lambda_{2E}^2 + \lambda_{3E}^2}} \quad \cos \alpha_E = \frac{+ \lambda_{3E}}{\sqrt{\lambda_{2E}^2 + \lambda_{3E}^2}} \quad (33)$$

and

$$\sin \alpha_P = \frac{- \lambda_{2P}}{\sqrt{\lambda_{2P}^2 + \lambda_{3P}^2}} \quad \cos \alpha_P = \frac{- \lambda_{3P}}{\sqrt{\lambda_{2P}^2 + \lambda_{3P}^2}} \quad (34)$$

These conditions may now be substituted into the state and costate equations to yield the TPBVP as functions of only the states and the costates themselves.

Linear Equation Development

As mentioned in Chapter II, the linear equation development involves both the pursuer and the evader almost from the beginning so the entire development was delayed until this time. Again there is the requirement to define state variables, r being the linearized, normalized state variables listed below.

$$\Delta x_{1E} = \frac{\Delta r_E}{r_0} \quad (35a)$$

$$\Delta x_{2E} = \frac{\Delta v_{rE}}{v_0} \quad (35b)$$

$$\Delta X_{3E} = \frac{\Delta V_{\theta E}}{V_0} \quad (35c)$$

$$\Delta X_{4E} = \Delta \theta \quad (35d)$$

A like set of terms exists for the pursuer with the subscript (E) replaced by (P).

In order to reduce the number of dimensions in this problem, it was necessary to combine the pursuer's and the evader's state variables into one difference relationship, now represented by the Y vector. Fig. 2 depicts the linearized parameters which have been combined into Y_1 and Y_4 .

The linearized, normalized state variables then become

$$Y_1 = \frac{\Delta X_{1E} - \Delta X_{1P}}{r_0} = \frac{\Delta r_E - \Delta r_P}{r_0} \quad (36a)$$

$$Y_2 = \frac{\Delta V_{rE} - \Delta V_{rP}}{V_0} \quad (36b)$$

$$Y_3 = \frac{\Delta V_{\theta E} - \Delta V_{\theta P}}{V_0} \quad (36c)$$

$$Y_4 = \Delta \theta_E - \Delta \theta_P \quad (36d)$$

Differentiating these equations with respect to τ by use of Eq. (12) and replacing the dotted terms by use of Eqs. (3) and (4) result in the following linearized state equations.

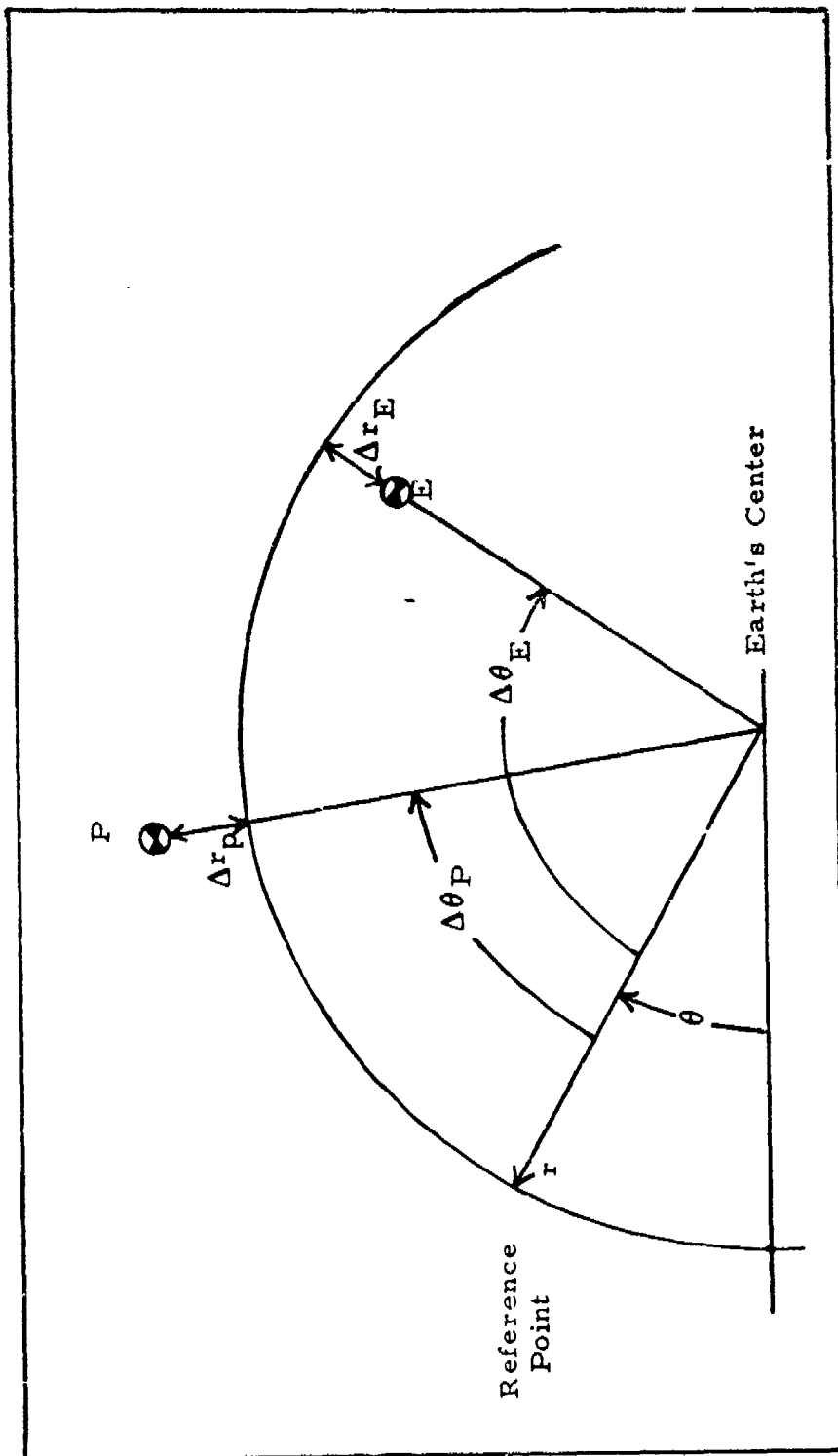


Fig. 2. Linearized Geometry

$$Y'_1 = \frac{r_0}{v_0} \frac{d}{dt} \left[\frac{\Delta r_E - \Delta r_P}{r_0} \right] = \frac{\Delta v_{rE} - \Delta v_{rP}}{v_0} = Y_2 \quad (37a)$$

$$Y'_2 = \frac{2r_0}{v_0^2} \left[\frac{v_{\theta E} \Delta v_{\theta E}}{v_0} - \frac{v_{\theta P} \Delta v_{\theta P}}{v_0} \right] + \frac{r_0}{v_0^2}$$

$$\left[\frac{v_{\theta E}^2 \Delta r_E}{r_E^2} - \frac{v_{\theta P}^2 \Delta r_E}{r_P^2} \right] + \frac{r_0}{v_0^2} \left[\frac{T_E \sin \alpha_E}{m_E} - \frac{T_P \sin \alpha_P}{m_P} \right] \quad (37b)$$

$$Y'_3 = -\frac{r_0}{v_0^2} \left[\frac{v_{\theta E} \Delta v_{rE}}{r_E} - \frac{v_{\theta P} \Delta v_{rP}}{r_P} \right] + \frac{r_0}{v_0^2}$$

$$\left[\frac{T_E \cos \alpha_E}{m_E} - \frac{T_P \cos \alpha_P}{m_P} \right] \quad (37c)$$

$$Y'_4 = \frac{r_0}{v_0} \left[\frac{\Delta v_{\theta E}}{r_E} - \frac{\Delta v_{\theta P}}{r_P} \right] - \frac{r_0}{v_0} \left[\frac{v_{\theta E} \Delta r_E}{r_E^2} - \frac{v_{\theta P} \Delta r_P}{r_P^2} \right] \quad (37d)$$

With the reference orbit identical to the normalizing orbit,

$$r = r_0$$

and

$$v_{\theta} = v_0$$

Using these expressions and by once again letting $U = \frac{r_0 T}{v_0^2 m}$, the above

equations reduce to the following state equations.

$$Y'_1 = Y_2 \quad (38a)$$

$$Y'_2 = 2Y_3 + Y_1 + U_E \sin \alpha_E - U_P \sin \alpha_P \quad (38b)$$

$$Y'_3 = -Y_2 + U_E \cos \alpha_E - U_P \cos \alpha_P \quad (38c)$$

$$Y'_4 = Y_3 - Y_1 \quad (38d)$$

These equations are now linear in state only, still being non-linear in the control angle α . They will, however, continue to be referred to as linear equations.

This development for the linear state equations again is similar to the work of R. H. Woodward (Ref. 3).

The Hamiltonian for the above equations is again formed by adjoining the costates to these state equations.

$$H = \Delta \lambda_1 Y_2 + \Delta \lambda_2 [2Y_3 + Y_1 + U_E \sin \alpha_E - U_P \sin \alpha_P] + \Delta \lambda_3 [-Y_2 + U_E \cos \alpha_E - U_P \cos \alpha_P] + \Delta \lambda_4 [Y_3 - Y_1] \quad (39)$$

By once again applying the necessary conditions of Eq. (20), the following costate equations are formed.

$$\Delta \lambda'_1 = -\frac{\partial H}{\partial Y_1} = -\Delta \lambda_2 + \Delta \lambda_4 \quad (40a)$$

$$\Delta \lambda'_2 = -\Delta \lambda_1 + \Delta \lambda_3 \quad (40b)$$

$$\Delta\lambda'_3 = -2\Delta\lambda_2 - \Delta\lambda_4 \quad (40c)$$

$$\Delta\lambda'_4 = 0 \text{ yielding } \Delta\lambda_4 = \text{a constant} \quad (40d)$$

The optimum thrust angles are found in the same manner as in the non-linear development yielding

$$\tan \alpha_E = \frac{\Delta\lambda_2}{\Delta\lambda_3} \quad (41)$$

and

$$\tan \alpha_P = \frac{\Delta\lambda_2}{\Delta\lambda_3} \quad (42)$$

By applying the second partial derivative relationships of Eqs. (30), the following optimum barrier control angles are determined.

$$\sin \alpha_E = \frac{+\Delta\lambda_2}{\sqrt{\Delta\lambda_2^2 + \Delta\lambda_3^2}} = \sin \alpha_P \quad (43)$$

$$\cos \alpha_E = \frac{+\Delta\lambda_3}{\sqrt{\Delta\lambda_2^2 + \Delta\lambda_3^2}} = \cos \alpha_P \quad (44)$$

These equations demonstrate that when both the pursuer and the evader play their optimal strategies, their thrust angles will be the same. On substituting these expressions into the state and costate equations, these equations reduce to a TPBVP again as functions of only the states and costates themselves.

Terminal Conditions

Non-linear Development. A circular terminal surface is assumed, lying in the plane containing the pursuer, the evader, and the center of the earth. This surface, then, provides the end conditions for certain state and costate equations. These conditions are determined from the following relationship representing the assumed terminal surface.

$$\frac{1}{2} \left[(x_{1E} - x_{1P})^2 + (x_{4E} - x_{4P})^2 - R^2 \right] = 0 \quad (45)$$

where

$$x_{1E} - x_{1P} = R \sin \phi \quad (46a)$$

and

$$x_{4E} - x_{4P} = R \cos \phi \quad (46b)$$

In this expression ϕ is defined as the angle around the terminal surface measured counterclockwise from the pursuer's local horizontal. The terminal surface and parameters are depicted in Fig. 3.

The vector \underline{v} mentioned previously as normal to the terminal surface is found by taking the gradient of Eq. (45). This operation yields the following terminal state and costate relationships.

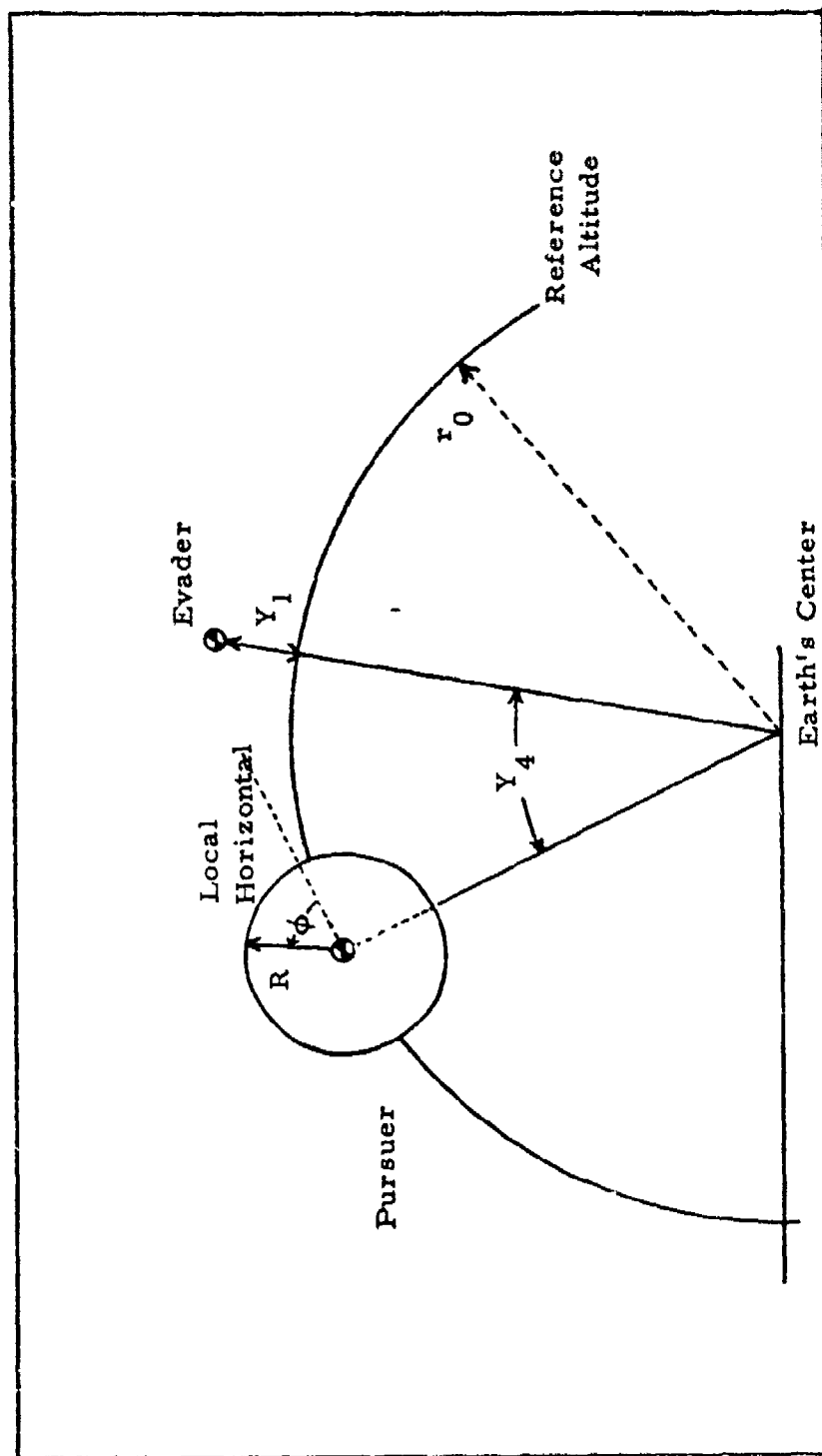


Fig. 3. Terminal Surface Parameters

$$\nabla [\text{Eq. (45)}] = \begin{bmatrix} \frac{x_{1E} - x_{1P}}{R} \\ \frac{x_{4E} - x_{4P}}{R} \\ \frac{x_{1P} - x_{1E}}{R} \\ \frac{x_{4P} - x_{4E}}{R} \end{bmatrix}_{t_f} = \begin{bmatrix} \lambda_{1E} \\ \lambda_{4E} \\ \lambda_{1P} \\ \lambda_{4P} \end{bmatrix}_{t_f} = \begin{bmatrix} \sin \phi \\ \cos \phi \\ -\sin \phi \\ -\cos \phi \end{bmatrix}$$

$$\text{as well as } \lambda_{2E}, \lambda_{3E}, \lambda_{2P}, \lambda_{3P} = 0 \quad (47)$$

Here, vector \underline{v} is represented by $\lambda_{1E}, \dots, \lambda_{4E}, \lambda_{1P}, \dots, \lambda_{4P}$.

The remainder of the terminal conditions may be found by using the condition for the boundary of the usable part, Eq. (26).

$$\begin{aligned} H_B = \underline{v} \cdot \underline{X} &= \lambda_{1E} x_{2E} + \lambda_{2E} \left[\frac{x_{3E}^2}{x_{1E}} - \frac{1}{x_{1E}^2} + U_E \sin \alpha_E \right] \\ &+ \lambda_{3E} \left[-\frac{x_{2E} x_{3E}}{x_{1E}} + U_E \cos \alpha_E \right] + \frac{\lambda_{4E} x_{3E}}{x_{1E}} + \lambda_{1P} x_{2P} \\ &+ \lambda_{2P} \left[\frac{x_{3P}^2}{x_{1P}} - \frac{1}{x_{1P}^2} + U_P \sin \alpha_P \right] + \lambda_{3P} \left[-\frac{x_{2P} x_{3P}}{x_{1P}} + U_P \cos \alpha_P \right] \\ &+ \frac{\lambda_{4P} x_{3P}}{x_{1P}} \end{aligned} \quad (48)$$

This equation is identical to the Hamiltonian of Eq. (28). Therefore, $H_B(t_f) = 0$ as in Eq. (25), and using the terminal conditions in Eq. (47), this reduces to

$$\left[X_{2E} - X_{2P} \right] \sin \phi + \left[\frac{X_{3E}}{X_{1E}} - \frac{X_{3P}}{X_{1P}} \right] \cos \phi = 0 \quad (49)$$

To determine the thrust angle values at the terminal surface, $\tan \alpha$ is evaluated.

$$\tan \alpha_E \Big|_{t_f} = \frac{\lambda_{2E}}{\lambda_{3E}} \Big|_{t_f} = \frac{0}{0}$$

This indeterminate form is solved by applying L'Hospital's Rule to yield

$$\tan \alpha_E \Big|_{t_f} = \frac{-\lambda_{1E} X_{1E}}{-\lambda_{4E}} \Big|_{t_f} = \frac{X_{1E} \sin \phi}{\cos \phi} = X_{1E} \tan \phi \quad (50)$$

or

$$\sin \alpha_E \Big|_{t_f} = -X_{1E} \sin \phi \quad (51a)$$

$$\cos \alpha_E \Big|_{t_f} = -\cos \phi \quad (51b)$$

Since $\sin \alpha_P$ and $\cos \alpha_P$ are just the negative of the α_E terms, the α_P terminal conditions are as follows.

$$\sin \alpha_P \Big|_{t_f} = X_{1P} \sin \phi \quad (52a)$$

$$\cos \alpha_P \Big|_{t_f} = \cos \phi \quad (52b)$$

Linear Development. Once again the terminal surface about the pursuer, P, is assumed to be circular, and the following relationship represents this surface.

$$\frac{1}{2} \left[Y_1^2 + Y_4^2 - R^2 \right] = 0 \quad (53)$$

where

$$Y_1 = R \sin \phi \quad (54a)$$

and

$$Y_4 = R \cos \phi \quad (54b)$$

with the angle ϕ representing the angle around the terminal surface measured counterclockwise from the pursuer's local horizontal.

Taking the gradient of Eq. (53) yields the following terminal relationships for the linear states and costates.

$$\nabla[\text{Eq. (53)}] = \begin{bmatrix} \frac{Y_1}{R} \\ 0 \\ 0 \\ \frac{Y_4}{R} \end{bmatrix}_{t_f} = \begin{bmatrix} \Delta \lambda_1 \\ \Delta \lambda_2 \\ \Delta \lambda_3 \\ \Delta \lambda_4 \end{bmatrix}_{t_f} = \begin{bmatrix} \sin \phi \\ 0 \\ 0 \\ \cos \phi \end{bmatrix} \quad (55)$$

The remaining conditions are determined by using Eq. (26) for the boundary of the usable part.

$$\begin{aligned}
 H_B &= \underline{v} \cdot \dot{\underline{x}} = \Delta\lambda_1 Y'_1 + \Delta\lambda_2 Y'_2 + \Delta\lambda_3 Y'_3 + \Delta\lambda_4 Y'_4 \\
 &= \Delta\lambda_1 Y_2 + \Delta\lambda_2 \left[2Y_3 + Y_1 + U_E \sin \alpha_E - U_P \sin \alpha_P \right] \\
 &\quad + \Delta\lambda_3 \left[-Y_2 + U_E \cos \alpha_E - U_P \cos \alpha_P \right] + \Delta\lambda_4 \left[Y_3 - Y_1 \right] \quad (56)
 \end{aligned}$$

This equation is identical to Eq. (39). From Eq. (25), then, $H_B(t_f) = 0$, and using the conditions in Eq. (55), this relationship reduces to

$$Y_2 \sin \phi + Y_3 \cos \phi - R \sin \phi \cos \phi = 0$$

or

$$Y_3 \Big|_{t_f} = R \sin \phi - Y_2 \tan \phi \Big|_{t_f} \quad (57)$$

To evaluate the thrust angle α at the terminal surface, where α_E is equal to α_P , it can be seen that

$$\tan \alpha_E \Big|_{t_f} = \frac{\Delta\lambda_2}{\Delta\lambda_3} \Big|_{t_f} = \frac{0}{0}$$

By applying L'Hospital's Rule, the value of α at the terminal surface is determined.

$$\tan \alpha \Big|_{t_f} = \tan \phi \quad (58a)$$

or

$$\alpha_E = \alpha_P = \phi \text{ at } t_f \quad (58b)$$

Both the pursuer's thrust angle and the angle around the terminal surface ϕ are measured from the pursuer's local horizontal. When the terminal surface has been reached, then, the pursuer would desire to have maximum velocity outward in order to force penetration by the evader, thus his thrust angle would equal ϕ . The evader, still attempting to avoid penetration, would obviously point his thrust in the same direction as the pursuer's thrust to neutralize the outward velocity of the pursuer.

IV. Methods of Solving the Linear Equations

In order to use the linear equations developed in the foregoing chapters to determine the barrier, it is necessary to find closed-form solutions to the state and costate equations. This chapter, then, presents the methods to use in finding these solutions.

The Costate Equations

These equations are to be used in backward integration, as mentioned previously in Chapter III. In order to do this, however, another time variable must be introduced which corresponds to t_f , the final time at the terminal surface. Define this backwards time as $\tau_1 = 0$ at t_f . In order to integrate backwards, the signs in the costate equations are reversed so that proper values may be obtained as the trajectory proceeds outward from the terminal surface. The linearized costate equations are repeated below with initial conditions at $\tau_1 = 0$ and with signs reversed for backward integration.

$$\Delta\lambda_1' = \Delta\lambda_2 - \Delta\lambda_4 \quad \Delta\lambda_1(\tau_1 = 0) = \frac{Y_1}{R} = \sin \phi \quad (59a)$$

$$\Delta\lambda_2' = \Delta\lambda_1 - \Delta\lambda_3 \quad \Delta\lambda_2(0) = 0 \quad (59b)$$

$$\Delta\lambda_3' = 2\Delta\lambda_2 + \Delta\lambda_4 \quad \Delta\lambda_3(0) = 0 \quad (59c)$$

$$\Delta\lambda_4' = 0 \text{ yielding } \Delta\lambda_4(\tau_1) = \text{a constant} = \Delta\lambda_4(0) = \cos \phi \quad (59d)$$

The solution to these equations is approached through $\Delta\lambda_2'$ by taking

another derivative with respect to τ in order to eliminate terms other than $\Delta\lambda_2$ and constants. This yields the following homogeneous solution.

$$\Delta\lambda_{2H} = A \sin \tau_1 + B \cos \tau_1 + C \quad (60)$$

By differentiating this expression twice and substituting back into the differential equation for $\Delta\lambda_2''$, the constant C may be found. By applying the initial conditions, constants A and B can also be found yielding the closed-form equation for $\Delta\lambda_2$ as a function of τ_1 .

$$\Delta\lambda_2(\tau_1) = \sin \phi \sin \tau_1 + 2 \cos \phi \cos \tau_1 - 2 \cos \phi \quad (61a)$$

By applying Eq. (61a) to Eqs. (59a) and (59c), the remainder of the closed-form $\Delta\lambda$ equations may be found.

$$\begin{aligned} \Delta\lambda_1(\tau_1) = & -\sin \phi \cos \tau_1 + 2 \cos \phi \sin \tau_1 - 3\tau_1 \cos \phi \\ & + 2 \sin \phi \end{aligned} \quad (61b)$$

$$\begin{aligned} \Delta\lambda_3(\tau_1) = & -2 \sin \phi \cos \tau_1 + 4 \cos \phi \sin \tau_1 - 3\tau_1 \cos \phi \\ & + 2 \sin \phi \end{aligned} \quad (61c)$$

$$\Delta\lambda_4(\tau_1) = \text{constant} = \cos \phi \quad (61d)$$

The State Equations

The state equations are solved in the same manner as were the costate equations. The state equations with initial conditions at $\tau_1 = 0$

and with signs reversed for backward integration are repeated below.

In these equations ϕ again represents the angle around the terminal surface measured counterclockwise from the pursuer's local horizontal.

$$Y'_1 = - Y_2 \quad Y_1(\tau_1 = 0) = R \sin \phi \quad (62a)$$

$$Y'_2 = - 2Y_3 - Y_1 - (U_E - U_P) \sin \alpha \quad (62b)$$

$$Y'_3 = Y_2 - (U_E - U_P) \cos \alpha \quad Y_3(0) = R \sin \phi - Y_2(0) \tan \phi \quad (62c)$$

$$Y'_4 = - Y_3 + Y_1 \quad Y_4(0) = R \cos \phi \quad (62d)$$

The closed-form solution to these linearized state equations is approached through Y'_2 ; however, to handle these equations, approximations for both $\sin \alpha$ and $\cos \alpha$ are required. The development of these approximations is presented in Appendix A with the following Taylor Series expressions in τ_1 for $\sin \alpha$ and $\cos \alpha$ resulting.

$$\sin \alpha = \pm \left[A - \frac{B}{2A} \tau_1 + \left(\frac{C}{A} - \frac{B^2}{4A^3} \right) \frac{\tau_1^2}{2} + \left(\frac{3BC}{2A^3} - \frac{3B^3}{8A^5} \right) \frac{\tau_1^3}{6} \right] \quad (63)$$

where

$$A = \sin \phi$$

$$B = 2 \sin \phi \cos \phi$$

$$C = - \frac{5}{6} + 2 \cos^2 \phi + \sin^2 \phi \cos^2 \phi$$

$$\cos \alpha = \pm \left[D + \frac{E}{2D} \tau_1 + \left(\frac{F}{D} - \frac{E^4}{4D^3} \right) \frac{\tau_1^2}{2} + \left(\frac{3E^3}{8D^5} - \frac{3EF}{2D^3} \right) \frac{\tau_1^3}{6} \right] \quad (64)$$

where

$$D = \cos \phi$$

$$E = 2 \sin \phi \cos \phi$$

$$F = \frac{5}{6} - 2 \cos^2 \phi - \sin^2 \phi \cos^2 \phi$$

The approximations for $\sin \alpha$ and $\cos \alpha$ are checked for accuracy in the equivalence section as part of the linear to non-linear comparison. There, when the negative sign is applied to both approximations, the resulting trajectories are found to be equivalent out to five decimal places up to a value comparable to twenty seconds off the terminal surface. In Appendix A these approximations are presented in a different form in order to more easily determine the solution to the state equations. By taking another derivative of Y_2' with respect to τ , the homogeneous solution is found to be

$$Y_{2H} = P \sin \tau_1 + Q \cos \tau_1 \quad (65)$$

Choosing a particular solution,

$$Y_{2P} = K_1 + K_2 \tau_1 + K_3 \tau_1^2 + K_4 \tau_1^3 \quad (66)$$

The total solution for Y_2 is then

$$Y_2 = P \sin \tau_1 + Q \cos \tau_1 + K_1 + K_2 \tau_1 + K_3 \tau_1^2 + K_4 \tau_1^3 \quad (67)$$

Allowing the difference in thrust constants to equal β ($\beta = U_E - U_P$) and applying the initial conditions, the constants may be evaluated. Rather than list these constants here, however, the entire solution is included in Appendix A.

By using the solution for Y_2 , the remainder of the state equations can be solved in closed-form with the constants again evaluated by applying the initial conditions at the terminal surface. The closed-form solutions to the state equations, then, are as follows.

$$Y_1 = P \cos \tau_1 - Q \sin \tau_1 - K_1 \tau_1 - \frac{K_2 \tau_1^2}{2} - \frac{K_3 \tau_1^3}{3} - \frac{K_4 \tau_1^4}{4} + MM \quad (68)$$

$$Y_3 = -P \cos \tau_1 + Q \sin \tau_1 + (K_1 + \beta A_2) \tau_1 + (K_2 + \beta B_2) \frac{\tau_1^2}{2} + (K_3 + \beta C_2) \frac{\tau_1^3}{3} + (K_4 + \beta D_2) \frac{\tau_1^4}{4} + N \quad (69)$$

$$Y_4 = 2 P \sin \tau_1 + 2 Q \cos \tau_1 - (2K_1 + \beta A_2) \frac{\tau_1^2}{2} - (2K_2 + \beta B_2) \frac{\tau_1^3}{6} - (2K_3 + \beta C_2) \frac{\tau_1^4}{12} - (2K_4 + \beta D_2) \frac{\tau_1^5}{20} + (MM - N) \tau_1 + S \quad (70)$$

Once again the constants are evaluated in Appendix A along with the entire solution to these equations.

V. Analysis of the Barrier

To analyze the barrier, trajectories must be generated outward from the terminal surface to provide points necessary for constructing the barrier itself. The method used in this thesis to generate these trajectories is that of backward integration. This method is easy to apply and results in numerous trajectories from the terminal surface. Although the analysis of these many trajectories may be tedious, backward integration avoids the difficulties of iteration methods while providing ample information on the barrier.

In applying the backward integration method, two computer programs are required, one for the linear and one for the non-linear equations. In order to use the closed-form solutions to the linear equations in analyzing the barrier, the linear trajectories must be equivalent to those generated by the non-linear computer program. [The area of equivalence will be discussed in a later section of this chapter.] After these trajectories are compared, linear to non-linear, the points on either side of the barrier, using the linear trajectories, must be analyzed to determine, where possible, whether they lie in the escape zone or the capture zone. This chapter, then, presents the linear and non-linear computer programs, the equivalence analysis, and the methods of determining whether escape or capture occurs from any given starting point.

The Linear Program

In developing the computer program to handle the linear state equations in closed form, a primary concern was the data to be used. In Chapter II the equations of motion of a satellite in orbit around the earth were linearized and normalized about a circular reference orbit. For this thesis the altitude of this reference orbit above the earth's surface was selected as 200 nautical miles, a height used in many manned orbital flights. On converting to the earth's canonical units, the radius r_0 of this orbit is 1.0581 distance units (DU) with a reference velocity V_0 of 0.97216 DU/TU, where TU is the earth's canonical time unit.

Since the initially specified variable Y_2 is the difference between the pursuer's and evader's radial velocities, which have been linearized and normalized about the 200 nautical mile reference orbit, the given value of $Y_2(0)$ at the terminal surface will have to be quite small. In order to gain equivalence between the linear and non-linear programs, an arbitrary value of $Y_2(0)$ was taken as 0.005. This value is equivalent in size to a relative velocity difference of approximately 130 feet per second. The value of $Y_2(0)$, however, could actually be varied while holding the other variables constant as an alternative in seeking more information about the shape of the barrier.

In conjunction with the arbitrary selection of $Y_2(0)$ is the selection of the value for the difference in normalized thrusts, $U_E - U_p$, labeled BT in the computer program. The numerical value of BT was

selected to give the pursuer a slight advantage since equal values of U_E and U_p would make $BT = 0$, thus removing the control from the solution. BT , then, was given the value - 0.04 reflecting the fact that the pursuer's thrust is greater than the evader's thrust. This value of normalized thrust difference resulted from applying thrusts of a magnitude equivalent to providing just over one-tenth- g of acceleration. With the value of BT specified, only the radius of the terminal surface R and the angle ϕ on that surface remain unspecified.

Since the value of ϕ will obviously vary around the terminal surface in establishing the boundary of the usable part, this term will remain as a variable to be changed readily in both programs. Since the radius of the terminal surface R is a non-dimensional quantity, its value must be selected in reference to the size of r_0 , the reference orbit radius. If the radius of the terminal surface were equivalent to 1000 ft, the value of the non-dimensional R would be 4.78×10^{-5} . With these values of ϕ and R , the initial conditions for the linear program were completely specified. These initial conditions were then applied to the closed-form solutions to the linear equations presented in Chapter IV to generate the required trajectories backward in time from the terminal surface. A sample of this computer program is included in Appendix B.

The Non-linear Program

For equivalence between the linear and non-linear programs,

data values comparable to those in the linear program must be selected. Here, however, eight initial values are necessary in order to completely specify the initial conditions due to the dimensionality of the non-linear program, whereas only four initial conditions were required in the linear program. The values for r_0 and V_0 are not considered as initial values since these are only used as references and are not specifically used in the programs. In determining these initial values, first of all consider the values that are common to both programs.

The values of R , ϕ , and BT would be the same as in the linear program with BT split into individual values of $U_E = 0.11$ and $U_P = 0.15$ giving the same difference, BT . The other common value is that of $Y_2(0)$, here representing again the difference between the players' radial velocities, assuming that the non-linear relative difference is approximately equal to the linear relative difference. The other values for this program are selected mostly from considering the previously given values.

The remaining values at termination to be specified are the pursuer's state variable initial conditions. Since the evader's initial conditions may be determined from these values, the pursuer's values are the only ones required. Eqs. (47) and (49) for the relationship of these initial conditions are repeated below for easy reference.

$$X_{1E} - X_{1P} = R \sin \phi \quad (47)$$

$$X_{4E} - X_{4P} = R \cos \phi$$

$$(X_{2E} - X_{2P}) \sin \phi + \left(\frac{X_{3E}}{X_{1E}} - \frac{X_{3P}}{X_{1P}} \right) \cos \phi = 0 \quad (49)$$

Since these values are to be determined at termination, the pursuer's values are arbitrarily assumed to approach the values of the reference orbit for easier handling. Therefore, the values of the normalized radius and tangential velocity will be one, and the value of the normalized radial velocity will be zero. This leaves the angle θ_P as the only unspecified value.

In selecting θ_P , the value of $Y_4 = \Delta\theta_E - \Delta\theta_P$ from the linear program was considered since it is presumed that $Y_4(0)$ will be equivalent to the difference between θ_E and θ_P from the non-linear program. Referring to Eqs. (47) and remembering that the magnitude of R is 4.78×10^{-5} , the value of $R \cos \phi$ and hence the difference in θ_E and θ_P will be quite small. The value of θ_P is then arbitrarily chosen to be 4×10^{-5} . This, then, completely specifies the data values for the non-linear program. Once again a sample of this program is presented in Appendix B for reference or future work.

Equivalence

Once the data values for both computer programs were established as of comparable magnitude, the trajectories produced by each

program were compared for equivalence. The search for equivalence started with attaining the proper values specified previously and with finding the proper step size for the non-dimensional time, T_1 . This quantity's numerical size was determined from the relationship, $T_1 = \frac{V_0 t}{r_0}$, where t is in time units. Since the canonical time unit is so large, the value of T_1 was successively reduced by a factor of one-tenth in searching for equivalence. At a step size of 0.001 the trajectory values from both the linear and non-linear programs came to within 2% of each other out to an equivalent of two hundred seconds off the terminal surface. Some of the values that were compared for the angle ϕ of 355 degrees are listed in Table I.

Both the linear programs, one for integration of the linear state and costate equations and one for the closed-form solution equations, were found to be equivalent out to a comparable value of at least two hundred seconds off the terminal surface. The importance of gaining equivalence for the closed-form equation trajectories lay in the desire to use these closed-form equations for analyzing the starting point locations. This analysis provides the final section in this chapter on analyzing the barrier.

Starting Point Locations

The analysis of the barrier was concluded by a search for a method of determining whether a given starting point lay in the escape zone or in the capture zone. This problem had to be approached

Table I
Equivalence Values, $\phi = 355$ Degrees

Non-linear Integration Values				
Y(1)	Y(2)	Y(3)	Y(4)	TAU ₁
-4.16629E-06	5.00000E-03	4.33303E-04	4.76181E-05	0.
-9.16400E-06	4.99549E-03	4.78149E-04	4.71557E-05	0.001
-5.39272E-05	4.95020E-03	8.81359E-04	4.07532E-05	0.01
-1.27482E-04	4.85243E-03	1.55153E-03	2.11428E-05	0.025
-2.46146E-04	4.62799E-03	2.66208E-03	-3.62128E-05	0.05
-3.58246E-04	4.32742E-03	3.76253E-03	-1.24075E-05	0.075
-4.61890E-04	3.95161E-03	4.85054E-03	-2.41966E-05	0.1
-5.55208E-04	3.50148E-03	5.92382E-03	-3.89311E-04	0.125
-6.36353E-04	2.97796E-03	6.98012E-03	-5.65437E-04	0.15
-7.03502E-04	2.38203E-03	8.01727E-03	-7.69576E-04	0.175
-7.54898E-04	1.71466E-03	9.03313E-03	-1.00087E-03	0.2

Linear Closed-Form Equation Values				
Y(1)	Y(2)	Y(3)	Y(4)	TAU ₁
-4.16629E-06	5.00000E-03	4.33303E-04	4.76181E-05	0.
-9.16410E-06	4.99559E-03	4.78147E-04	4.71557E-05	0.001
-5.39281E-05	4.95027E-03	8.81361E-04	4.07532E-05	0.01
-1.27482E-04	4.85223E-03	1.55160E-03	2.11405E-05	0.025
-2.46126E-04	4.62626E-03	2.66231E-03	-3.62340E-05	0.05
-3.58148E-04	4.32272E-03	3.76275E-03	-1.24141E-05	0.075
-4.61630E-04	3.94338E-03	4.85025E-03	-2.42100E-05	0.1
-5.54709E-04	3.49109E-03	5.92221E-03	-3.89519E-04	0.125
-6.35609E-04	2.96983E-03	6.97608E-03	-5.65694E-04	0.15
-7.02668E-04	2.38468E-03	8.00946E-03	-7.69817E-04	0.175
-7.54362E-04	1.74182E-03	9.02005E-03	-1.00098E-03	0.2

through the linear, closed-form solution equations as mentioned previously. Since the barrier is defined in terms of four dimensions in three parameters, the method of specifying starting point locations had to be completely analytical through use of the linear equations. Also, since time limitations precluded any extensive examination of this method, this development really results in a theoretical method for considering given starting points near the barrier.

The approach to discovering a method to locate given starting points in relation to the barrier was to find a normal to the barrier surface which would pass through the given point. In three-dimensional surfaces the normal is based on the orthogonality of the coordinate system in which the surface is presented. Since the four coordinates of this thesis are also orthogonal, the three-dimensional normal theory was extended to handle the four-dimensional barrier surface that was found in this study.

The normal to a four-dimensional surface was formulated from the three-dimensional development of R. C. Buck (Ref 6:335). In this reference the normal to a three-dimensional surface as a function of two parameters, u and v , was found as follows.

$$\underline{n} = \left[\frac{d(y, z)}{d(u, v)}, \frac{d(z, x)}{d(u, v)}, \frac{d(x, y)}{d(u, v)} \right]$$

To extend this equation from three dimensions in two parameters to four dimensions with three parameters: ϕ , $Y_2(0)$, and T_1 , the following normal equation was proposed.

$$\underline{N} = \left[\frac{d(Y_2, Y_3, Y_4)}{d(\phi, Y_2(0), \tau_1)}, \frac{d(Y_3, Y_4, Y_1)}{d(\phi, Y_2(0), \tau_1)}, \frac{d(Y_4, Y_1, Y_2)}{d(\phi, Y_2(0), \tau_1)}, \frac{d(Y_1, Y_2, Y_3)}{d(\phi, Y_2(0), \tau_1)} \right] \quad (71)$$

In this equation the Y-terms refer to Eqs. (67) through (70), the linear, closed-form solution equations. By evaluating the four, three-by-three determinants in Eq. (71), the normal at any point on the barrier may be determined. Due to the complexity of these determinants, it was not deemed beneficial to list the final equation form for this four-dimensional barrier. The easiest method of dealing with the normal would be to take the partial derivatives of the Y-equations with respect to the three parameters and evaluate these at a point along the barrier. Once all the partial derivatives for a given point have been evaluated, the determinants, and thus the normal itself, could be determined.

Once the normal has been determined, the obvious question deals with where the given point off the barrier is in relation to the barrier. On generating normals all along the barrier, one will surely pass through the given starting point or point exactly opposite to the direction through the given point. By taking the dot product between any normal vector and the vector from the base of that normal to the given point, the angle between the two vectors may be found. By searching in the four coordinate directions, it should be possible to find the point on the barrier where the normal passes through the given starting point or 180 degrees away from the point. Knowing this would tell whether the point was on the positive or negative side of the barrier and, therefore, in the capture or escape zone respectively.

VI. Conclusions and Recommendations

Conclusions

The objective of this study was to determine a differential game barrier for a pursuit-evasion game between two spacecraft in orbit. Throughout the chapters of this thesis, this general area of concern was broken down into smaller sections dealing with the search for this barrier. These sections dealt with the development of the linear and non-linear state and costate equations, the theory of differential game barriers, and finally an analysis of the barrier itself.

The state and costate equations were used to generate trajectories backward in time from the terminal surface. These trajectories were then compared, linear to non-linear, and once equivalence had been verified, the barrier for this problem was determined. However, this barrier was a four-dimensional surface that depended on three parameters: ϕ , $Y_2(0)$, and τ_1 . With $\tau_1 = 0$ at the terminal surface, one specified set of values for ϕ and $Y_2(0)$ established a unique boundary of the usable part in four space. This is obviously difficult to demonstrate graphically; however, by making a ratio of the relative velocities, Y_2/Y_3 , a three-dimensional presentation of the barrier is possible. Figures 4 through 7, then, portray the boundary of the usable part in the four quadrants of a cylindrical terminal surface. Along with the boundary of the usable part in Fig. 4 is a portion of the barrier itself out to a value equivalent to one and one-half seconds off

MC/GA/73A-3

$Y_2/Y_3 \times 10^2$

$Y_1 \times 10^5$

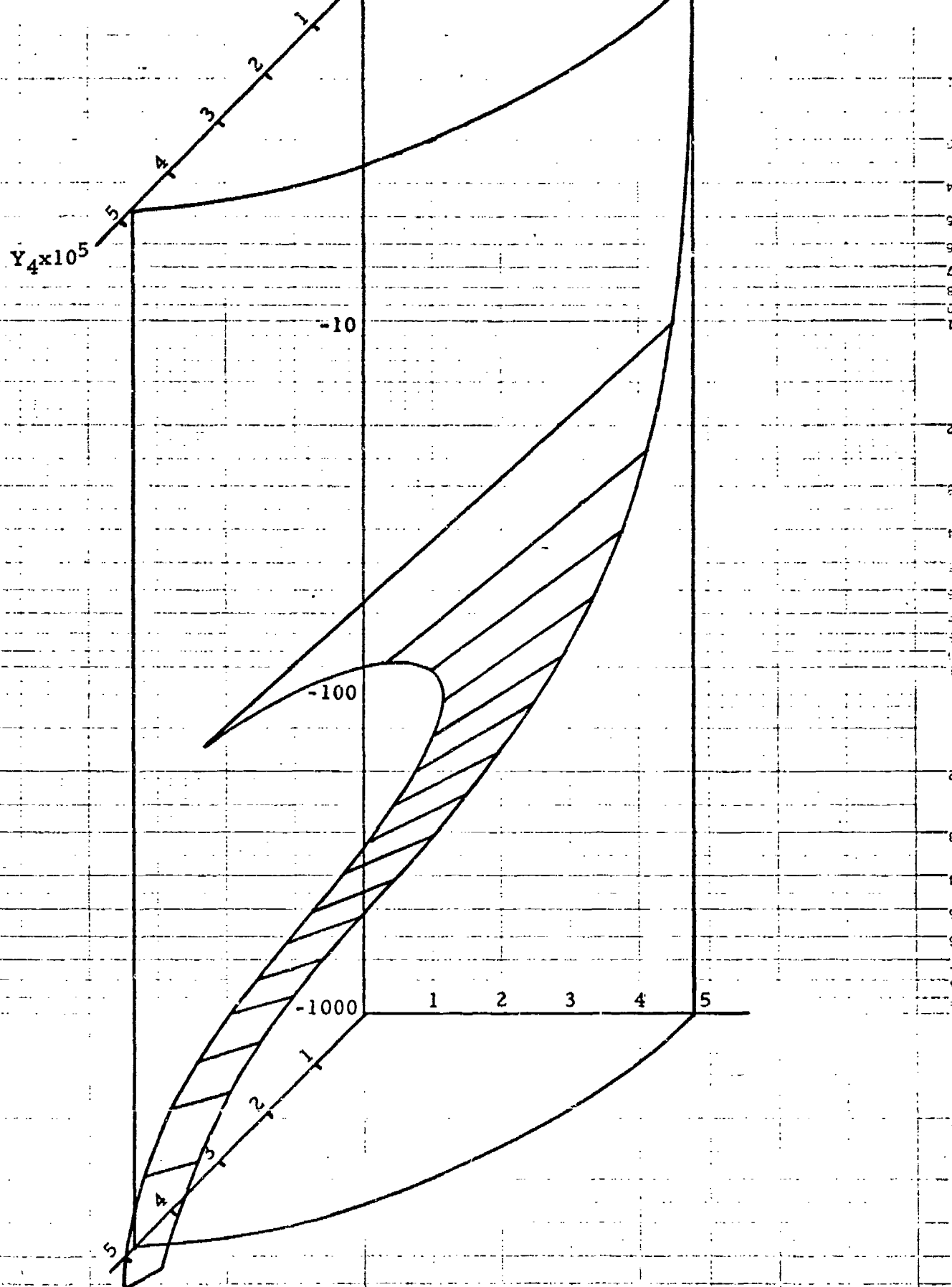


Fig. 4. Boundary of the Usable Part and Barrier Portion,
0 to 90 Degrees

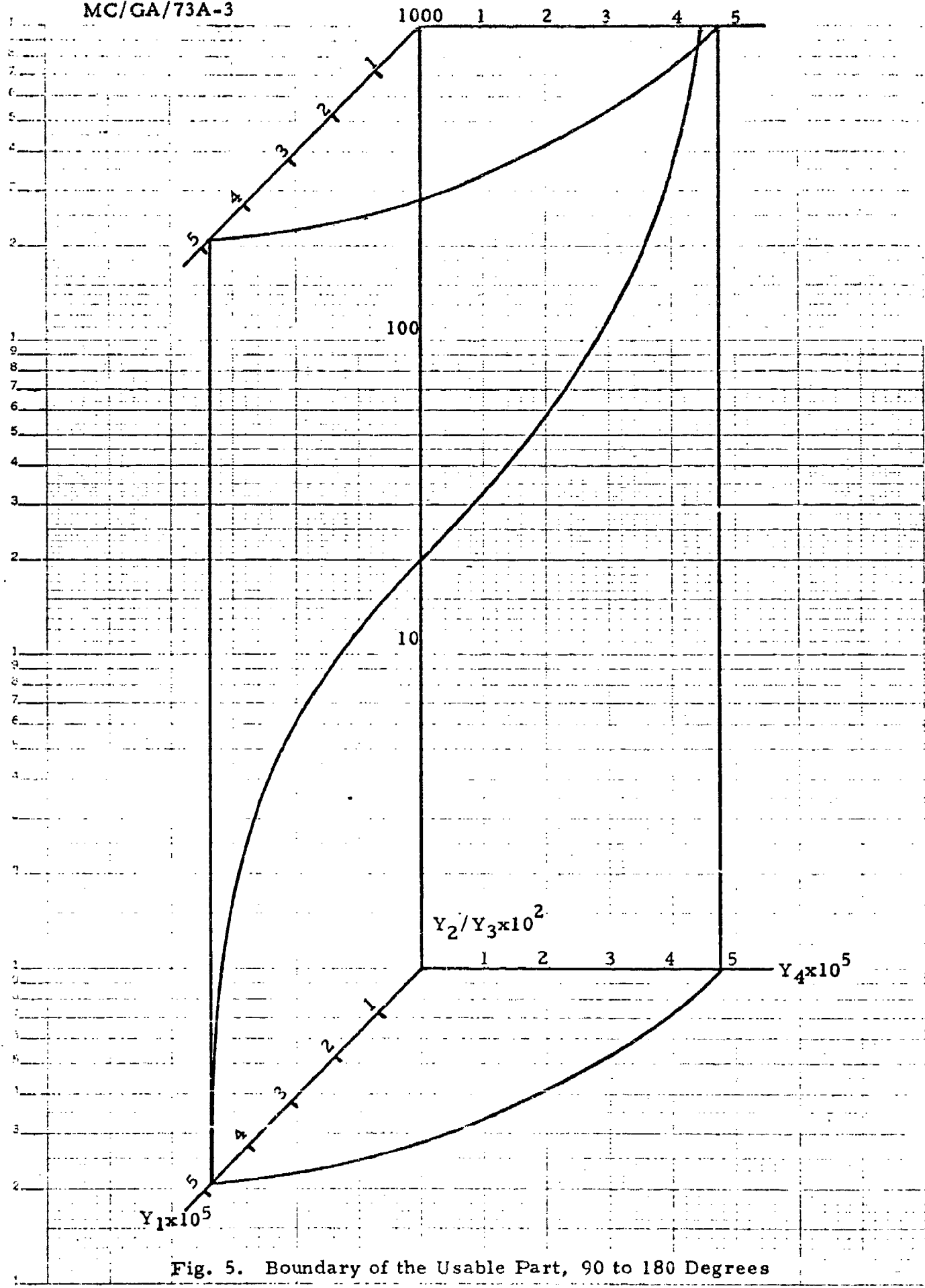


Fig. 5. Boundary of the Usable Part, 90 to 180 Degrees

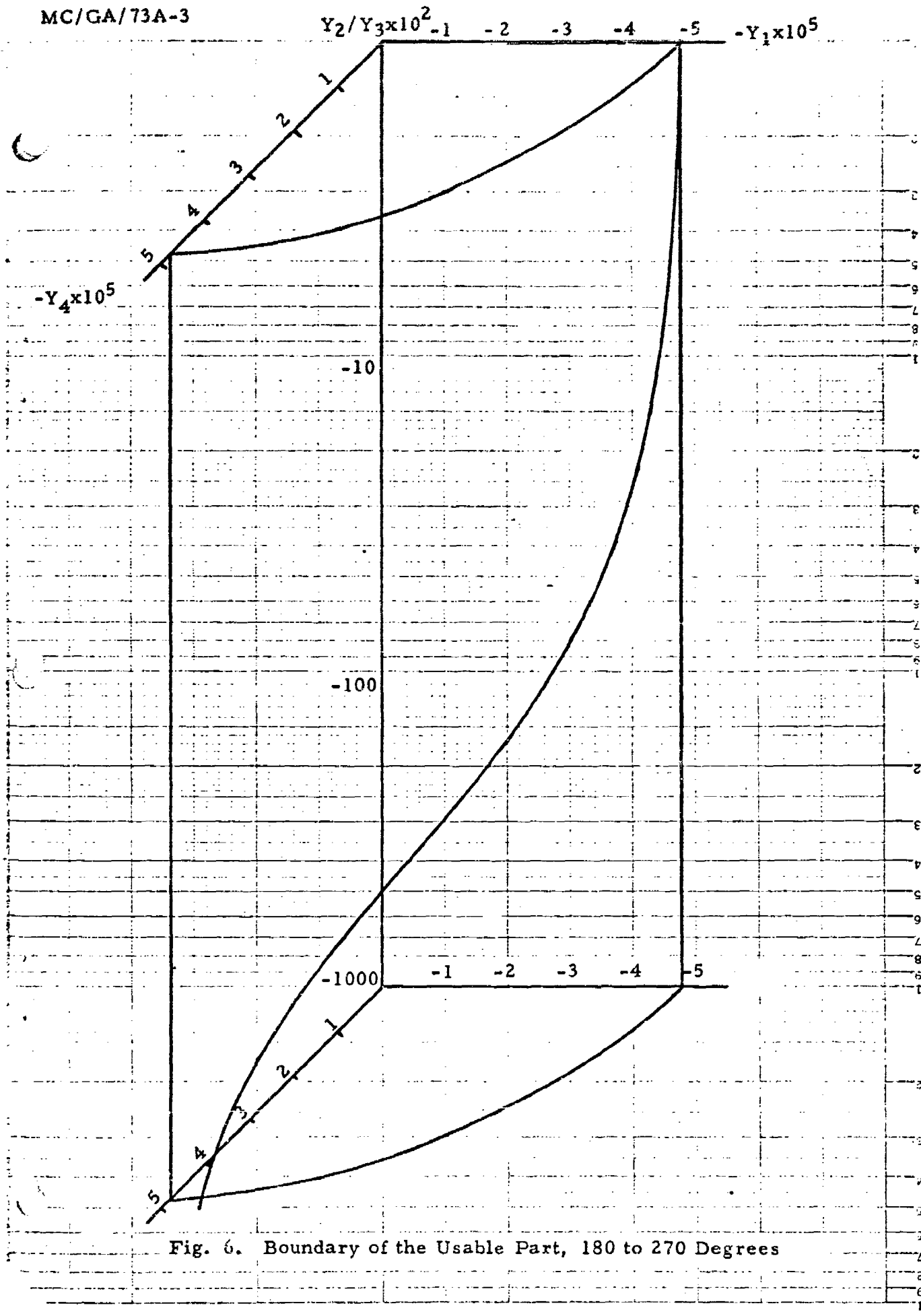


Fig. 6. Boundary of the Usable Part, 180 to 270 Degrees

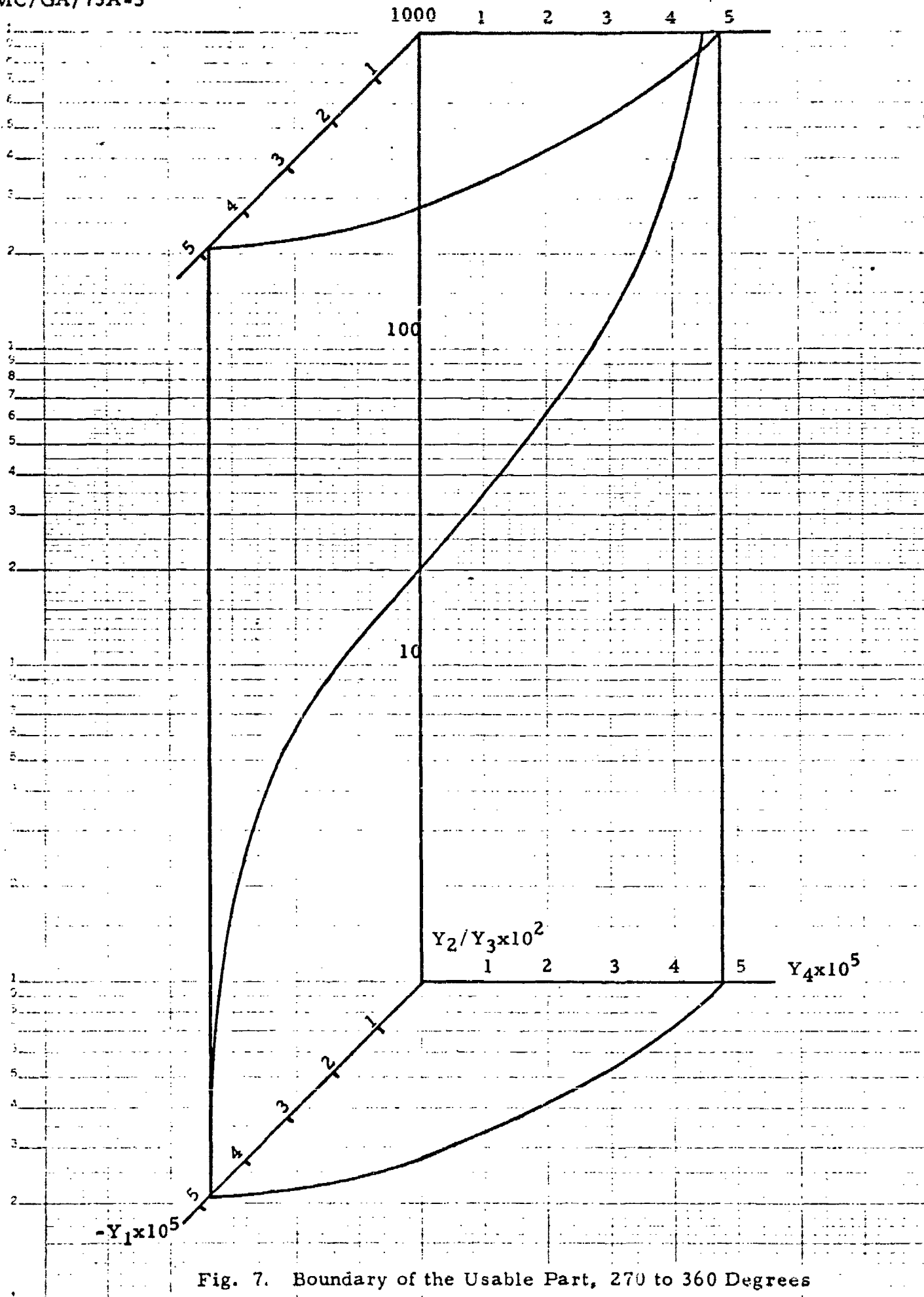


Fig. 7. Boundary of the Usable Part, 270 to 360 Degrees

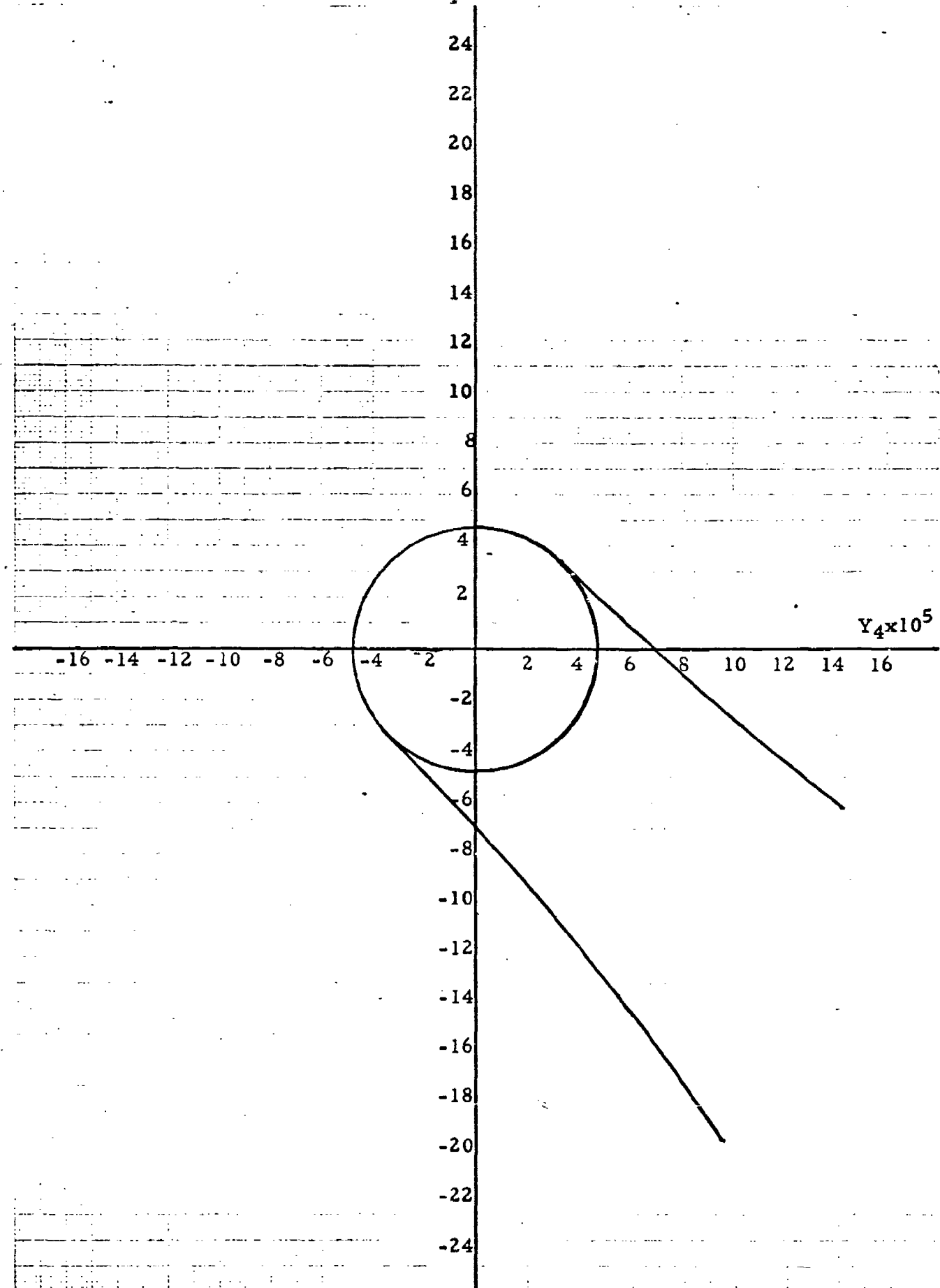
the terminal surface. To better present this barrier, two planes were passed through the cylinder parallel to the plane containing Y_1 and Y_4 at values of Y_2/Y_3 equal to plus and minus one hundred in the scale of Fig. 4. These two-dimensional barrier segments out to an equivalent of twenty seconds off the terminal surface are shown in Figures 8 and 9.

Once the barrier was determined, then, meeting the main objective of this study, the barrier itself was analyzed to determine the location of various starting points lying just off the barrier. A theoretical presentation of a method to determine these locations was presented in the last chapter. Time limitations, however, precluded a complete evaluation of this method, as mentioned previously; therefore, this portion of the objective was only partially completed.

Recommendations

The first and most obvious recommendation would be to extend the analysis of the barrier to determine the location of starting points in the playing space lying just off the barrier. Since the linear, closed-form equations have been checked for accuracy with the non-linear equations, these linear equations provide a ready starting point for this further analysis. Once the technique for determining the normal to a four-dimensional barrier surface has been evaluated, the location of the given starting points could be determined.

Another area for further study would be to extend the analysis

Fig. 8. Barrier Cut at $Y_2/Y_3 = -1.00$

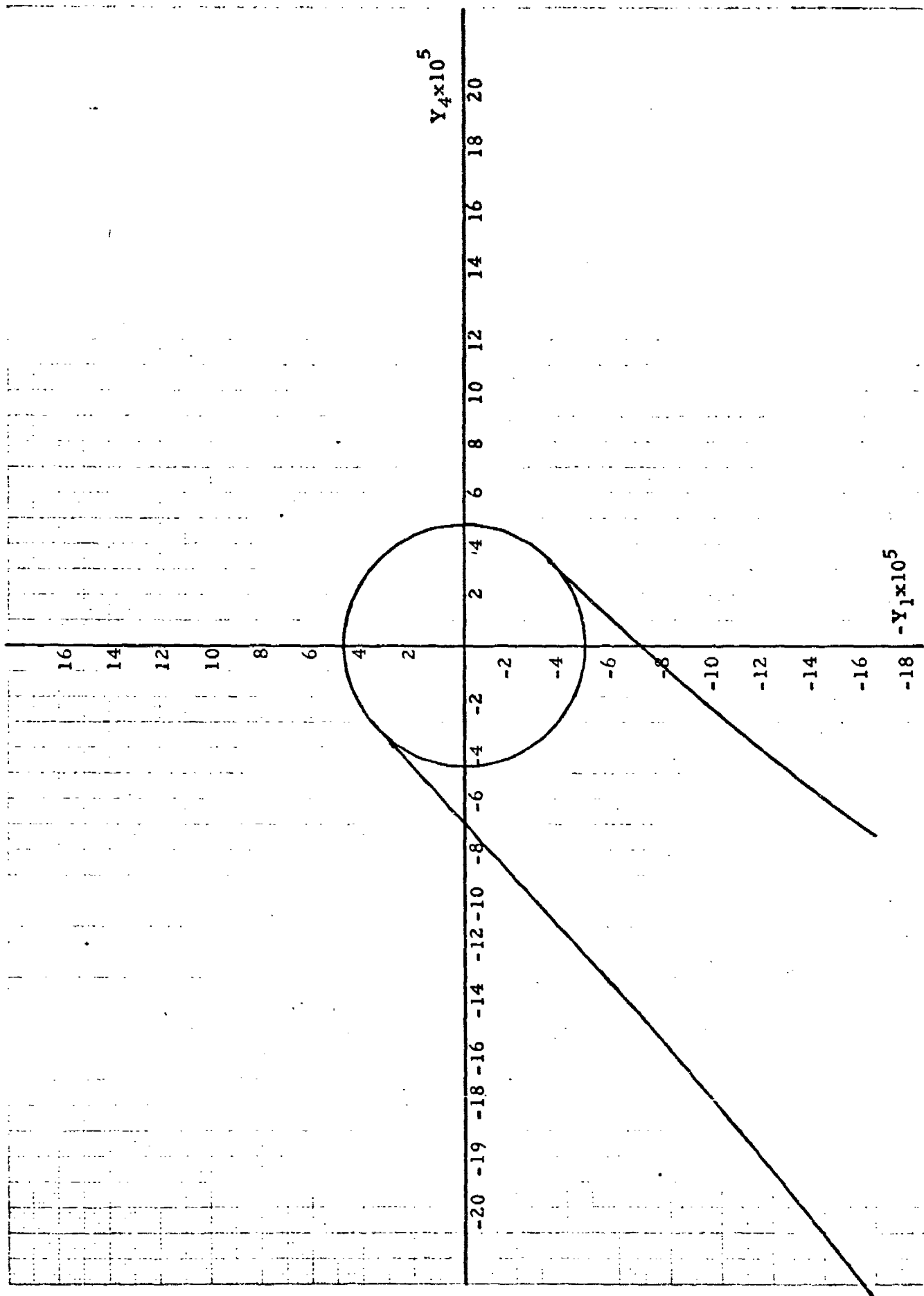


Fig. 9. Barrier Cut at $Y_2/Y_3 = +1.00$

of the barrier in three dimensions. By making more cuts along the Y_2/Y_3 axis, the barrier could be completely defined allowing graphical analysis along with the above mentioned analytic analysis. In addition to this recommendation would be one to vary the value of $Y_2(0)$, the relative velocity difference in the radial direction at the terminal surface. This would generate a changing barrier surface which could provide information concerning the velocity requirements for either capture or escape.

Bibliography

1. Isaacs, Rufus. A Mathematical Theory with Applications to Warfare and Pursuit, Control and Optimization. New York: John Wiley and Sons, Inc., 1965.
2. Wong, R. E. "Some Aerospace Differential Games." Journal of Spacecraft and Rockets, 4: 1460-1465 (November 1967).
3. Woodward, Richard H. Pursuit-Evasion Games Between Two Spacecraft in Near-Earth Orbit. Unpublished Thesis. Wright-Patterson Air Force Base, Ohio: Air Force Institute of Technology, March 1972.
4. Bryson, A. E. and Y. Ho. Applied Optimal Control. Waltham, Massachusetts: Blaisdell Company, 1969.
5. Cawdery, P. H. Toward the Definition of Escape and Capture Regions for a Two Aircraft Pursuit-Evasion Game. Unpublished Thesis. Wright-Patterson Air Force Base, Ohio: Air Force Institute of Technology, June 1973.
6. Buck, R. Creighton. Advanced Calculus. New York: McGraw-Hill Book Company, 1965.

Appendix ASine and Cosine Approximations

In order to use the state equations effectively, it is necessary to get the $\sin \alpha$ and $\cos \alpha$ terms into expressions that can be solved. This requires expanding the expressions for $\sin \alpha$ and $\cos \alpha$ in Taylor Series expansions about the point $\tau_1 = 0$, where τ_1 is the non-dimensional, backward integrating time. In the linear equations, as stated in Chapter III, the optimal control angles for the pursuer and the evader were found to be equal; therefore, only two approximations, one for the sine and one for the cosine, are necessary. Since

$$\sin \alpha = \frac{\Delta \lambda_2}{\sqrt{\Delta \lambda_2^2 + \Delta \lambda_3^2}} \quad (72)$$

it was necessary to first square this expression before expanding. This results in an equation of the form

$$\sin^2 \alpha = \frac{\Delta \lambda_2^2}{\Delta \lambda_2^2 + \Delta \lambda_3^2} = \frac{f(\phi, \tau_1)}{g(\phi, \tau_1)} \quad (73)$$

This is readily expanded in the following manner, assuming that τ_1 is small.

$$\sin^2 \alpha = \frac{f(\phi, \tau_1)}{g(\phi, \tau_1)} \Bigg|_{\tau_1=0} + \left[\frac{\frac{df}{d\tau_1}}{g} - \frac{f \frac{dg}{d\tau_1}}{g^2} \right]_{\tau_1=0} \tau_1 + \frac{1}{2} \left[\frac{\frac{d^2 f}{d\tau_1^2}}{g} - \frac{2 \frac{df}{d\tau_1} \frac{dg}{d\tau_1}}{g^2} \right. \\ \left. - \frac{\frac{d^2 g}{d\tau_1^2}}{g^2} + \frac{2f \left(\frac{dg}{d\tau_1} \right)^2}{g^3} \right]_{\tau_1=0} \tau_1^2 \quad (74)$$

where

$$f(\phi, \tau_1) = \sin^2 \phi \sin^2 \tau_1 + 4 \cos^2 \phi \cos^2 \tau_1 + 4 \cos^2 \phi \\ + 4 \sin \phi \cos \phi \sin \tau_1 \cos \tau_1 - 4 \sin \phi \cos \phi \sin \tau_1 - 8 \cos^2 \phi \cos \tau_1 \quad (75a)$$

and

$$g(\phi, \tau_1) = 4 + 4 \cos^2 \tau_1 + 12 \sin \phi \cos \phi \sin \tau_1 - 12 \sin \phi \cos \phi \sin \tau_1 \cos \tau_1 \\ + \sin^2 \phi \sin^2 \tau_1 - 8 \cos \tau_1 + 16 \cos^2 \phi \sin^2 \tau_1 + 9 \tau_1^2 \cos^2 \phi \\ + 12 \tau_1 \sin \phi \cos \phi \cos \tau_1 - 24 \tau_1 \cos^2 \phi \sin \tau_1 - 12 \tau_1 \sin \phi \cos \phi \quad (75b)$$

At $\tau_1 = 0$, these terms reduce to zero. By taking derivatives of f and g with respect to τ_1 and then evaluating at $\tau_1 = 0$, the following expressions result.

$$\left. \frac{df}{d\tau_1} \right|_{\tau_1=0} = 0 \quad (75c)$$

$$\left. \frac{d^2 f}{d\tau_1^2} \right|_{\tau_1=0} = 2 \sin^2 \phi \quad (75d)$$

$$\left. \frac{d^3 f}{d r_1^3} \right|_{r_1=0} = -12 \sin \phi \cos \phi \quad (75e)$$

$$\left. \frac{d^4 f}{d r_1^4} \right|_{r_1=0} = -8 + 32 \cos^2 \phi \quad (75f)$$

$$\left. \frac{dg}{d r_1} \right|_{r_1=0} = 0 \quad (75g)$$

$$\left. \frac{d^2 g}{d r_1^2} \right|_{r_1=0} = 2 \quad (75h)$$

$$\left. \frac{d^3 g}{d r_1^3} \right|_{r_1=0} = 0 \quad (75i)$$

$$\left. \frac{d^4 g}{d r_1^4} \right|_{r_1=0} = 16 - 24 \cos^2 \phi \quad (75j)$$

The first term in Eq. (74) is then

$$\left. \frac{f(\phi, r_1)}{g(\phi, r_1)} \right|_{r_1=0} = \frac{0}{0}$$

Applying L'Hospital's Rule twice to this indeterminate expression yields the following relationship.

$$\left. \frac{\frac{d^2 f}{d r_1^2}}{\frac{d^2 g}{d r_1^2}} \right|_{r_1=0} = \sin^2 \phi \quad (75)$$

This then is the first coefficient of Eq. (74). The second coefficient is approached in the same manner after putting the expression over a common denominator.

$$\left[\frac{g \frac{df}{dr_1} - f \frac{dg}{dr_1}}{g^2} \right]_{r_1=0} = \frac{0}{0} \quad (77)$$

Applying L'Hospital's Rule four times finally results in

$$\frac{d^4}{dr_1^4} \left[g \frac{df}{dr_1} - f \frac{dg}{dr_1} \right] = 2 \frac{d^2 g}{dr_1^2} \frac{d^3 f}{dr_1^3} \quad (78a)$$

and

$$\frac{d^4}{dr_1^4} \left[g^2 \right] = 6 \left(\frac{d^2 g}{dr_1^2} \right)^2 \quad (78b)$$

At $r_1 = 0$, Eq. (78a) equals $-48 \sin \phi \cos \phi$ and Eq. (78b) equals 24 to yield the second coefficient for Eq. (74).

$$\left[\frac{g \frac{df}{dr_1} - f \frac{dg}{dr_1}}{g^2} \right]_{r_1=0} = -2 \sin \phi \cos \phi \quad (79)$$

The third coefficient of Eq. (74) is also put over a common denominator giving this expression.

$$\frac{1}{2} \left[\frac{g^2 \frac{d^2 f}{dr_1^2} - 2g \frac{df}{dr_1} \frac{dg}{dr_1} - g f \frac{d^2 g}{dr_1^2} + 2f \left(\frac{dg}{dr_1} \right)^2}{g^3} \right]_{r_1=0} = \frac{0}{0} \quad (80)$$

By applying L'Hospital's Rule six times as before and evaluating at

$T_1 = 0$, the third coefficient of Eq. (74) is determined to be

$$\frac{1}{2} \left[\frac{\frac{d^2 f}{dT_1^2}}{g} - \frac{2 \frac{df}{dT_1} \frac{dg}{dT_1}}{g^2} - \frac{f \frac{d^2 g}{dT_1^2}}{g^2} + \frac{2f \left[\frac{dg}{dT_1} \right]^2}{g^3} \right]_{T_1=0} =$$

$$- \frac{5}{6} + 2 \cos^2 \phi + \sin^2 \phi \cos^2 \phi \quad (81)$$

Substituting the results of Eqs. (76), (79), and (81) into Eq. (74) yields the following expression for $\sin \alpha$.

$$\sin \alpha = \pm \left[\sin^2 \phi - (2 \sin \phi \cos \phi) T_1 + \left(-\frac{5}{6} + 2 \cos^2 \phi + \sin^2 \phi \cos^2 \phi \right) T_1^2 \right]^{1/2} \quad (82)$$

Since this expression is actually the square root of the function, another approximation is required. The above expression, then, is expanded in a Taylor Series expansion about $T_1 = 0$ as follows, the coefficients of T_1 being lumped into constants for ease of handling.

$$F(T_1) = (A^2 - B T_1 + C T_1^2)^{1/2} \quad F(0) = A$$

$$F'(T_1) = \frac{1}{2} (A^2 - B T_1 + C T_1^2)^{-1/2} (-B + 2C T_1) \quad F'(0) = \frac{-B}{2A}$$

$$F''(\tau_1) = -\frac{1}{4} (A^2 - B\tau_1 + C\tau_1^2)^{-3/2} (-B + 2C\tau_1)^2 + C(A^2 - B\tau_1 + C\tau_1^2)^{-1/2}$$

$$F''(0) = \frac{-B^2}{4A^3} + \frac{C}{A}$$

$$F'''(\tau_1) = \frac{3}{8} (A^2 - B\tau_1 + C\tau_1^2)^{-5/2} (-B + 2C\tau_1)^3 - (A^2 - B\tau_1 + C\tau_1^2)^{-3/2} (-B + 2C\tau_1)(C)$$

$$- \frac{C}{2} (A^2 - B\tau_1 + C\tau_1^2)^{-3/2} (-B + 2C\tau_1)$$

$$F'''(0) = \frac{3BC}{2A^3} - \frac{3B^3}{8A^5}$$

Therefore,

$$\sin \alpha = \pm \left[A - \frac{B}{2A} \tau_1 + \left(\frac{C}{A} - \frac{B^2}{4A^3} \right) \frac{\tau_1^2}{2} + \left(\frac{3BC}{2A^3} - \frac{3B^3}{8A^5} \right) \frac{\tau_1^3}{6} \right] \quad (83a)$$

where

$$A = \sin \phi \quad (83b)$$

$$B = 2 \sin \phi \cos \phi \quad (83c)$$

$$C = -\frac{5}{6} + 2 \cos^2 \phi + \sin^2 \phi \cos^2 \phi \quad (83d)$$

In a similar manner as above, the $\cos \alpha$ approximation is determined; however, in this case the identity $\cos^2 \alpha = 1 - \sin^2 \alpha$ is used. From this, an expansion of the square root is accomplished as before yielding the following $\cos \alpha$ approximation.

$$\cos \alpha = \pm \left[D + \frac{E}{2D} \tau_1 + \left(\frac{F}{D} - \frac{E^2}{4D^3} \right) \frac{\tau_1^2}{2} + \left(\frac{3E^3}{8D^5} - \frac{3EF}{2D^3} \right) \frac{\tau_1^3}{6} \right] \quad (84a)$$

where

$$D = \cos \phi \quad (84b)$$

$$E = 2 \sin \phi \cos \phi \quad (84c)$$

$$F = \frac{5}{6} - 2 \cos^2 \phi - \sin^2 \phi \cos^2 \phi \quad (84d)$$

Linear State Equation Solution

The linear state equations from Chapter III are repeated below for easy reference with the signs reversed for backward integration and with the determined initial conditions.

$$Y_1' = - Y_2 \quad Y_1(\mathcal{T}_1 = 0) = R \sin \phi \quad (85a)$$

$$Y_2' = - 2Y_3 - Y_1 - \beta \sin \alpha \quad (85b)$$

$$Y_3' = Y_2 - \beta \cos \alpha \quad Y_3(0) = R \sin \phi - Y_2(0) \tan \phi \quad (85c)$$

$$Y_4' = - Y_3 + Y_1 \quad Y_4(0) = R \cos \phi \quad (85d)$$

In these equations, $\beta = U_E - U_P$, the difference in normalized thrusts, \mathcal{T}_1 is the non-dimensional time for backward integration, and ϕ is the angle around the terminal surface measured counterclockwise from the pursuer's local horizontal. Rather than immediately use the approximations for $\sin \alpha$ and $\cos \alpha$ from the first section of this appendix, a new set of constants is selected. In making this selection the proper sign of Eqs. (83a) and (84a) had to be chosen. Only after the equivalence analysis was completed were the proper signs known; therefore, the following expressions are negative in order for

equivalence to occur between the non-linear and linear, closed-form computer programs.

$$\sin \alpha = - (A_1 + B_1 T_1 + C_1 T_1^2 + D_1 T_1^3) \quad (86a)$$

where

$$A_1 = A \quad (86b)$$

$$B_1 = \frac{-B}{2A} \quad (86c)$$

$$C_1 = \frac{1}{2} \left(\frac{C}{A} - \frac{B^2}{4A^3} \right) \quad (86d)$$

$$D_1 = \frac{1}{6} \left(\frac{3BC}{2A^3} - \frac{3B^3}{8A^5} \right) \quad (86e)$$

and

$$\cos \alpha = - (A_2 + B_2 T_1 + C_2 T_1^2 + D_2 T_1^3) \quad (87a)$$

where

$$A_2 = D \quad (87b)$$

$$B_2 = \frac{E}{2D} \quad (87c)$$

$$C_2 = \frac{1}{2} \left(\frac{F}{D} - \frac{E^2}{4D^3} \right) \quad (87d)$$

$$D_2 = \frac{1}{6} \left(\frac{3E^3}{8D^5} - \frac{3EF}{2D^3} \right) \quad (87e)$$

The constants A through F come from the first section of this appendix where they are evaluated.

By differentiating Y_2' again with respect to T and substituting in from the other state equations, an equation relating Y_2 terms and constants results.

$$Y_2'' + Y_2 = -2\beta(A_2 + B_2T_1 + C_2T_1^2 + D_2T_1^3) + \beta(B_1 + 2C_1T_1 + 3D_1T_1^2) \quad (88)$$

or

$$Y_2_H = P \sin T_1 + Q \cos T_1 \quad (89)$$

Choosing now a particular solution to the above equation,

$$Y_2_P = K_1 + K_2T_1 + K_3T_1^2 + K_4T_1^3 \quad (90)$$

and differentiating with respect to T_1 the constants K_1 through K_4 may be evaluated.

$$2K_3 + 6K_4T_1 + K_1 + K_2T_1 + K_3T_1^2 + K_4T_1^3 = -\beta[(2A_2 - B_1) + (2B_2 - 2C_1)T_1 + (2C_2 - 3D_1)T_1^2 + 2D_2T_1^3] \quad (91)$$

$$K_1 = -\beta(2A_2 + 6D_1 - B_1 - 4C_2) \quad (92a)$$

$$K_2 = -\beta(2B_2 - 2C_1 - 12D_1) \quad (92b)$$

$$K_3 = -\beta(2C_2 - 3D_1) \quad (92c)$$

$$K_4 = -2\beta D_2 \quad (92d)$$

This yields the following total solution for Y_2 :

$$Y_2 = Y_{2H} + Y_{2P} = P \sin T_1 + Q \cos T_1 + K_1 + K_2 T_1 + K_3 T_1^2 + K_4 T_1^3 \quad (93)$$

By use of the initial conditions in Eqs. (85) the constants P and Q may be determined.

$$Y_2 (T_1 = 0) = Q + K_1 \quad (94)$$

Therefore,

$$Q = Y_2(0) + \beta (2A_2 + 6D_1 - B_1 - 4C_2) \quad (95)$$

and

$$Y_2'(0) = P + K_2 = -3R \sin \phi + 2Y_2(0) \tan \phi - \beta \sin \phi \quad (96)$$

or

$$P = (-3R - \beta) \sin \phi + 2Y_2(0) \tan \phi + \beta (2B_2 - 2C_1 - 12D_2) \quad (97)$$

where $Y_2(0)$ is a specified initial condition for this thesis.

By using Eq. (93), the remainder of the closed-form solutions to the linear state equations may be found.

$$Y_1' = -P \sin T_1 - Q \cos T_1 - K_1 - K_2 T_1 - K_3 T_1^2 - K_4 T_1^3 \quad (98)$$

$$Y_1 = P \cos T_1 - Q \sin T_1 - K_1 T_1 - \frac{K_2 T_1^2}{2} - \frac{K_3 T_1^3}{3} - \frac{K_4 T_1^4}{4} + MM \quad (99)$$

where MM is determined by use of the initial conditions to be

$$MM = (4R + \beta) \sin \phi - 2Y_2(0) \tan \phi - \beta (2B_2 - 2C_1 - 12D_2) \quad (100)$$

$$Y_3 = -P \cos \mathbf{T}_1 + Q \sin \mathbf{T}_1 + K_1 \mathbf{T}_1 + \frac{K_2 \mathbf{T}_1^2}{2} + \frac{K_3 \mathbf{T}_1^3}{3} + \frac{K_4 \mathbf{T}_1^4}{4} + \beta \left(A_2 \mathbf{T}_1 + \frac{B_2 \mathbf{T}_1^2}{2} + \frac{C_2 \mathbf{T}_1^3}{3} + \frac{D_2 \mathbf{T}_1^4}{4} \right) + N \quad (101)$$

where

$$N = (-2R - \beta) \sin \phi + Y_2(0) \tan \phi + \beta (2B_2 - 2C_1 - 12D_2) \quad (102)$$

$$Y_4 = 2P \sin \mathbf{T}_1 + 2Q \cos \mathbf{T}_1 - (2K_1 + \beta A_2) \frac{\mathbf{T}_1^2}{2} - (2K_2 + \beta B_2) \frac{\mathbf{T}_1^3}{6} - (2K_3 + \beta C_2) \frac{\mathbf{T}_1^4}{12} - (2K_4 + \beta D_2) \frac{\mathbf{T}_1^5}{20} + (MM - N) \mathbf{T}_1 + S \quad (103)$$

where

$$S = R \cos \phi - 2Y_2(0) - 2\beta (2A_2 + 6D_1 - B_1 - 4C_2) \quad (104)$$

Appendix BNon-linear Integration Program

```

PROGRAM NCNLIN(INPUT,CUTFLT,TAFE5=INPUT,TAFE6=OUTPUT)
DIMENSION XE(4),XP(4),CXE(4),EXP(4),LDAE(4),LDAP(4),LDLDAE(3),
1 CLDAP(3),XEAvg(4),LEAvg(3),XFAvg(4),LPAve(3),Y(4),SXE(4),
2 SXP(4),SCXE(4),SDXF(4),SCLCE(3),SOLDP(3),SLE(3),SLP(3)
REAL LDAE,LDAP,LEAvg,LPAve
READ(5,10) FEE,R,XP(1),XF(2),XP(3),XP(4)
10 FFORMAT(EE11.5)
READ(5,11) V0,R0,TAU,LE,UF
11 FORMAT(EE11.5)
READ(5,12) LDAE(2),LCAE(3),LCAP(2),LDAP(3)
12 FFORMAT(4E11.5)
WRITE(6,500)
500 FFORMAT(*T*)
13 PHI = (FEE*3.14159)/180.
TANPHI = SIN(PHI)/COS(PHI)
LCAE(1) = SIN(PHI)
LCAE(4) = COS(PHI)
LCAP(1) = -SIN(PHI)
LCAP(4) = -COS(PHI)
WRITE(6,20)
20 FFORMAT(*      PHI          R          XP(1)          XP(2)
1          XP(3)          XF(4)          TAU *)
1 WRITE(6,21) FEE,R,XF(1),XF(2),XP(3),XP(4),TAU
21 FFORMAT(1P7E15.5)
CT=7.0001
M=0
N=1
XE(1) = R*SIN(PHI)+XF(1)
XE(2)=Y20+XP(2)
XE(3)=R*SIN(PHI)-(XE(2)-XF(2))*TANPHI+XF(3)
XE(4) = R*COS(PHI)+XF(4)
Y(1)=XE(1)-XP(1)
Y(2)=XE(2)-XP(2)
Y(3)=XE(3)-XP(3)
Y(4)=(XE(4)-XF(4))
RTS=SQRT(Y(1)**2+Y(4)**2)
VTCT=SQRT(Y(2)**2+Y(3)**2)
VRAT=Y(2)/Y(3)
WRITE(6,110)
110 FFORMAT(*      Y(1)          Y(2)          Y(3)          Y(4)
1          RTS          Y(2)/Y(3)          VTCT          TAU*)
1 WRITE(6,25) Y(1),Y(2),Y(3),Y(4),RTS,VRAT,VTCT,TAU
25 FFORMAT(1P8E15.5)
150 IF(TAU.GT.0.) GC TO 101
CXE(2)=-(XE(3)**2/XE(1)-1./XE(1)**2-UF*XE(1)*SIN(PHI))
CXE(3)=--(-XF(2)*XE(3)/XE(1)+LE*COS(PHI))
CXF(2)=-(XP(3)**2/XF(1)-1./XF(1)**2+UF*XF(1)*(+SIN(PHI)))
CXF(3)=--(-XP(2)*XP(3)/XP(1)+UF*(+COS(PHI)))
GC TO 102

```

MC/GA/73A-3

```

101  DXE(2)=- (XE(3)**2/XE(1)-1./XE(1)**2+UE*LCAE(2)/(SQRT(LDAE(2)**2
    1 +LDAE(3)**2)))
    - DXE(3)=- (-XE(2)*XE(3)/XE(1)+LE*LDAE(3)/(SQRT(LDAE(2)**2+LDAE(3
    1 **2)))
    CXF(2)=- (XP(3)**2/XF(1)-1./XF(1)**2+UP*LCAF(2)/(SQRT(LDAP(2)**2
    1 +LDAP(3)**2)))
    CXF(3)=- (-XP(2)*XP(3)/XF(1)-LF*LDAP(3)/(SQRT(LDAP(2)**2+LDAF(3
    1 **2)))
102  CXF(1)=-XE(2)
    CXE(4)=-XE(3)/XE(1)
    CXP(1)=-XP(2)
    CXP(4)=-XP(3)/XF(1)
    CLCAE(1)=- ((LCAE(2)*XF(3)**2)/XE(1)**2-2.*LCAE(2)/XE(1)**3
    1 -(LDAE(3)*XE(2)*XE(3))/XE(1)**2+LDAE(4)*XE(3)/XE(1)**2)
    CLCAE(2)=- (-LCAE(1)+LCAE(3)*XE(3)/XE(1))
    CLCAF(3)=- (- (2.*LDAE(2)*XF(3))/XE(1)+LDAE(3)*XE(2)/XE(1)-LDAE(4
    1 /XE(1))
    CLCAF(1)=- ((LCAP(2)*XP(3)**2)/XP(1)**2-2.*LCAP(2)/XP(1)**3
    1 -(LDAP(3)*XP(2)*XP(3))/XF(1)**2+LDAP(4)*XF(3)/XF(1)**2)
    CLCAP(2)=- (-LCAP(1)+LCAF(3)*XF(3)/XP(1))
    CLCAF(3)=- (- (2.*LDAF(2)*XF(3))/XP(1)+LDAF(3)*XP(2)/XP(1)-LCAP(4
    1 /XP(1))
    IF (N.EG.1) GO TO 40
    CC 31 I=1,4
    SXE(I)=XE(I)
    SXF(I)=XF(I)
    SCXE(I)=DXE(I)
30    SCXP(I)=DXP(I)
    CC 31 I1=1,3
    SLE(I1)=LCAE(I1)
    SLF(I1)=LCAP(I1)
    SCLDE(I1)=DLDAE(I1)
    SCLDP(I1)=DLdap(I1)
    CC 32 I2=1,4
    XE(I2)=XE(I2)+DXE(I2)*DT
    32    XF(I2)=XF(I2)+DXF(I2)*DT
    CC 33 I?=1,3
    LCAE(I3)=LDAE(I3)+DLCAE(I3)*DT
    33    LCAP(I3)=LDAF(I3)+DLCAF(I3)*DT
    M=1
    CC TO 101
    40    CC 41 J=1,4
    XEAVG(J)=(SDXE(J)+DXF(J))/2.
    41    XFAVG(J)=(SDXF(J)+DXF(J))/2.
    CC 42 J1=1,3
    LEAVG(J1)=(SCLDE(J1)+DLDAE(-1))/2.
    42    LFAVG(J1)=(SCLDP(J1)+DLCAF(-1))/2.
    CC 50 K=1,4
    XE(K)=SXE(K)+XEAVG(K)*DT
    50    XF(K)=SXP(K)+XFAVG(K)*DT
    CC 51 K1=1,3
    LCAE(K1)=SLE(K1)+LEAVG(K1)*DT
    51    LCAP(K1)=SLP(K1)+LFAVG(K1)*DT
    IF (N.EG.100) GO TO FJ
    N=N+1
    M=M
    CC TO 101

```

```
60    Y(1)=(XE(1)-XP(1))
      Y(2)=(XF(2)-XP(2))
      Y(3)=(XE(3)-XP(3))
      Y(4)=(XF(4)-XP(4))
      RTS=SQRT(Y(1)**2+Y(4)**2)
      VFRAT=Y(2)/Y(3)
      VTOT=SQRT(Y(2)**2+Y(3)**2)
      TAU=TAU+0.001
      WRITE(6,26) Y(1),Y(2),Y(3),Y(4),RTS,VFRAT,VTOT,TAU
26    FFORMAT(1F8E15.5)
      IF(TAU.GT.3.02) GO TO 70
      M=0
      N=1
      GO TO 100
70    IF(FEE.LT.356.) GO TO 80
      FEE=FEE-5.
      TAU=0.
      XF(1)=1.
      XF(2)=0.
      XF(3)=1.
      XF(4)=0.0004
      GO TO 13
80    CONTINUE
      WRITE(6,501)
501    FFORMAT(*S*)
      END
```

Linear Integration Program

```

PROGRAM MAIN (INPUT,CLTFLT,TAPES=INPUT,TAPEE=OUTPUTPLT)
DIMENSION Y(4),PY(4),SY(4),SCY(4),LDA(4),CLDA(3),YAVG(4),
1 LDAVG(3),SLCA(3),SCLCA(3)
REAL LCA,LDAVG
READ (5,100) FFLT,Y20,R,ET,TAU
100 FORMAT (5E12.5)
WRITE (6,500)
500 FORMAT (*T*)
L=1
63 IF (L.EQ.73) GO TO 66
M=1
FFI=(FFE*3.14159)/180.
TANPHI=SIN(FFI)/COS(FFI)
LCA(1)= SIN(FFI)
LCA(2)= 0.
LCA(3)= 0.
LCA(4)= COS(FFI)
WRITE (6,10)
10 FORMAT (*      PHI      -      Y20      R      ET
1          TAU*)
1  WRITE (6,11) FFE,Y20,R,ET,TAU
11 FORMAT (1P8E15.5)
CT=0,JJ001
M=0
N=1
Y(1)=R*SIN(FFI)
Y(2)=Y20
Y(3)=R*SIN(FFI)-Y20*TANFFI
Y(4)=R*COS(FFI)
WRITE (6,11)
110 FORMAT (*      Y(1)      Y(2)      Y(3)      Y(4)
1          RTS      Y(2)/Y(3)      VTCT      TAU
1  RTS=SQRT(Y(1)**2+Y(4)**2)
VRAT=Y(2)/Y(3)
VTCT=SQRT(Y(2)**2+Y(3)**2)
WRITE (6,20) Y(1),Y(2),Y(3),Y(4),RTS,VRAT,VTCT,TAU
20 FORMAT (1P8E15.5)
101 IF (TAU.GT.0.) GO TO 102
CY(2)= -2.*Y(3)-Y(1)+ET*SIN(FFI)
CY(3)= Y(2)+ET*COS(FFI)
GO TO 103
102 CY(2)= -2.*Y(3)-Y(1)-RT*(LCA(2)/(SQRT(LCA(2)**2+LCA(3)**2)))
CY(3)= Y(2)-ET*(LCA(3)/(SCFT(LCA(2)**2+LCA(3)**2)))
103 CY(1)= -Y(2)
CY(4)= -Y(3)+Y(1)
CLDA(1)= LDA(2)-LDA(4)
CLDA(2)= LDA(1)-LDA(3)
CLDA(3)= 2.*LDA(2)+LDA(4)
IF (M.EQ.1) GO TO 40
DO 30 I=1,4
SY(I)= Y(I)
30 SCY(I)=0Y(I)

```

MC/GA/73A-3

```
CC 31 I1=1,3
SLOA(I1)= LCA(I1)
31 SELDA(I1)= DLOA(I1)
CC 32 I2=1,4
32 Y(I2)= Y(I2)+DY(I2)*DT
CC 33 I3=1,3
33 LDA(I3)= LDA(I3)+DLEA(I3)*CT
M=1
GC TO 102
41 CC 41 J=1,4
+1 YAVG(J)=(SDY(J)+DY(J))/2.
CC 42 J1=1,3
42 LCAVG(J1)=(SELDA(J1)+DLEA(J1))/2.
CC 50 J2=1,4
50 Y(J2)= SY(J2)+YAVG(J2)*CT
CC 51 J3=1,3
51 LCA(J3)= SLEA(J3)+LCAVG(J3)*CT
IF (N.EQ.10) GO TO 60
N=N+1
M=2
GC TO 102
50 RTS= SQRT(Y(1)**2+Y(4)**2)
VRAT=Y(2)/Y(3)
VTOT= SQRT(Y(2)**2+Y(3)**2)-
TAU=TAU+0.0001
WRITE (6,90) Y(1),Y(2),Y(3),Y(4),RTS,VRAT,VTOT,TAU
90 FFORMAT (1P8E15.5)
IF (MM.EQ.2) GO TO 70
M=0
N=1
MM=MM+1
CC TO 101
70 FEE=FEE-5.
TAU=0.
L=L+1
GC TO 63
66 CONTINUE
WRITE (6,501)
501 FFORMAT (*S*)
END
```

Linear Closed-Form Equation Program

```

PROGRAM MAIN (INPUT,CUTFLT,TAFES=INPUT,TAFEE=OUTPUT)
REAL K1,K2,K3,K4,MM,N
READ (5,100) FEE,Y20,R,ET,FC,TAU
100 FORMAT (F8.10)
L=1
53 IF (L.E0.2) GO TO 68
FFI= (FEE*3.14159)/180.
TANPHI=SIN(FFI)/COS(FFI)
AA = SIN(PHI)
EE = 2.*SIN(FFI)*COS(FFI)
CC = -5./6.+2.*COS(FFI)**2+SIN(PHI)**2*COS(FFI)**2
DD = COS(PHI)
A1 = -AA
P1 = +DD
C1 = -(CC/AA-B2**2/(4.*AA**3))/2.
E1 = -(3.*BB*CC)/(2.*AA**3)-(3.*BB**3)/(8.*AA**5))/6.
A2 = -DD
B2 = -BB/(2.*DD)
C2 = -(-CC/DD-BB**2/(4.*EE**3))/2.
E2 = -(3.*BB**3)/(8.*EE**5)+(3.*BB*CC)/(2.*EE**3))/6.
K1 = -(2.*A2-B1-4.*C2+6.*C1)*ET
K2 = -(2.*B2-2.*C1-12.*D2)*ET
K3 = -(2.*C2-3.*C1)*ET
K4 = -(2.*D2)*ET
G = Y20-K1
F = -(3.*R+RT)*AA+2.*TANPHI*Y20-K2
MM = (4.*R+RT)*AA-2.*Y20*TANPHI+K2
N = -(2.*R+RT)*AA+TANPHI*Y20-K2
S = R*DD-2.*Y20+2.*K1
WRITE (5,109)
109 FORMAT (*      PHI          Y20          ?          ET
1 *)
WRITE (5,110) FEE,Y20,F,ET
110 FORMAT (1F4T15.5)
WRITE (5,129)
129 FORMAT (*      Y1          Y2          Y3          Y4
1           RTS          Y2/Y3          TAU*)
M=1
64 IF (M.E0.21) GO TO 65
T=TAU
T1=TAU
Y1= P*COS(T1)-0*SIN(T1)-K1*T-K2*T**2/2.-K3*T**3/3.-K4*T**4/4.
1 +MM
Y2=P*SIN(T1)+Q*COS(T1)+K1+K2*T+K3*T**2+K4*T**3
Y3=-P*COS(T1)+Q*SIN(T1)+(K1+ET*A2)*T+(K2+ET*B2)*T**2/2.
1 +(K3+ET*C2)*T**3/3.+(K4+ET*D2)*T**4/4.+N
Y4=2.*F*SIN(T1)+2.*C*COS(T1)-(2.*K1+ET*A2)*T**2/2.-(2.*K2
1 +ET*B2)*T**3/3.-(2.*K3+ET*C2)*T**4/4.-(2.*K4+ET*D2)
2 *T**5/2.+(MM+N)*T+S
RTS=SQRT(Y1**2+Y4**2)
RATY23=Y2/Y3
VTOT=SQRT(Y2**2+Y3**2)

```

MC/GA/73A-3

```
      WRITE (6,137) Y1,Y2,Y3,Y4,RTS,RTATY23,TAL,VTOT
130  FORMAT (1P8E15.5)
      M=M+1
      TAU=TAU+0.011
      GO TO 64
65   CONTINUE
      TAU = 0.
      FEE=FEE-5.
      L=L+1
      GO TO 63
66   CONTINUE
      END
```

Vita

Victor W. Grazier was born on 29 April 1942 in Torrance, California. He graduated from Yreka High School in Yreka, California, in 1960. After one year at the Naval Preparatory School in Bainbridge, Maryland, he attended the United States Air Force Academy in Colorado Springs, Colorado, and graduated in 1965 with a Bachelor of Science degree in Engineering Sciences. After graduation and commissioning, he completed both Undergraduate Navigator Training and Navigator Bombardier Training at Mather Air Force Base, California. Following seven years of flying as a navigator in the EB-66 in such places as Takhli, Thailand; Shaw Air Force Base, South Carolina; and Spangdahlem Air Base, West Germany; he entered the Graduate Astronautics program at the Air Force Institute of Technology School of Engineering.

This thesis was typed by Mrs. Joyce A. Clark.